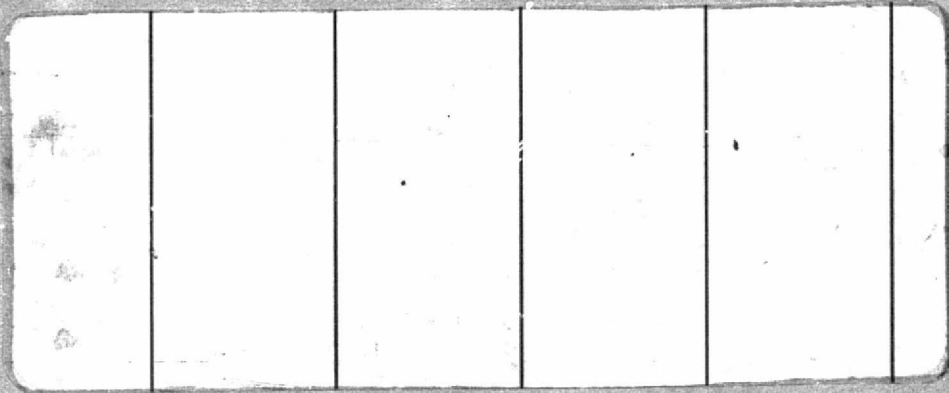


General Disclaimer

One or more of the Following Statements may affect this Document

- This document has been reproduced from the best copy furnished by the organizational source. It is being released in the interest of making available as much information as possible.
- This document may contain data, which exceeds the sheet parameters. It was furnished in this condition by the organizational source and is the best copy available.
- This document may contain tone-on-tone or color graphs, charts and/or pictures, which have been reproduced in black and white.
- This document is paginated as submitted by the original source.
- Portions of this document are not fully legible due to the historical nature of some of the material. However, it is the best reproduction available from the original submission.



(NASA-CR-144023)	DEFINITION OF THROW-AWAY	N76-11322
DETECTORS (TADS) AND VLF ANTENNA FOR THE		
AMPS LABORATORY Interim Report, 25 Feb. -		
26 Sep. 1975 (Aerospace Corp., El Segundo,		Unclas
Calif.) 119 p HC \$5.50	CSCL 17B G3/32	03032



THE AEROSPACE CORPORATION



Aerospace Report No.
ATR-76(7520)-1

INTERIM REPORT
DEFINITION OF THROW-AWAY DETECTORS (TADS)
AND VLF ANTENNA FOR THE AMPS LABORATORY

Prepared by
H. C. Koons and J. F. Fennell

26 SEPT 75

Space Physics Laboratory
Laboratory Operations
THE AEROSPACE CORPORATION
El Segundo, California 90245

Prepared for
GEORGE C. MARSHALL SPACE FLIGHT CENTER
Marshall Space Flight Center, Alabama 35812
Contract Number NAS8-31399

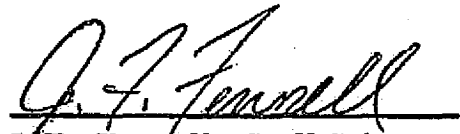
INTERIM REPORT:

DEFINITION OF THROW-AWAY DETECTORS (TADS) AND
VLF ANTENNA FOR THE AMPS LABORATORY

Prepared



H. C. Koons, Staff Scientist
Space Particles and Fields
Department

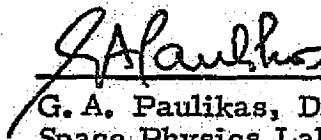


J. F. Fennell, Staff Scientist
Space Particles and Fields
Department

Approved



J. B. Blake, Head
Space Particles and Fields
Department



G. A. Paulikas, Director
Space Physics Laboratory
Laboratory Operations

FOREWORD

This report, which documents studies carried out from 25 February 1975 to 26 September 1975, is issued by The Aerospace Corporation, El Segundo, California. It is an Interim Report on studies conducted under NASA Contract Number NAS8-31399.

This contract provided support for studies to define scientific instruments which would be used on small, inexpensive subsatellites known as TADS and to define support required by these instruments and the method of providing this support. These TADS would initially be used to map the EMI and particulate environment around the Space Shuttle Orbiter to assess the impact of the environment on AMPS and other payloads.

This contract also provided support to review and assess the VLF antennas required to perform VLF transmission experiments from AMPS. The effort included a review of the theory of antenna performance in a space plasma, a review of previous experiments, and a definition of the hardware required to perform VLF experiments from AMPS.

The results of these studies are described in this report. The Report is divided into two independent parts, the TADS Study and the VLF Antenna Study.

CONTENTS

	Page
1.0 INTRODUCTION	1
1.1 Overview of Instruments for TAD/subsatellites . . .	1
1.2 Items to be Studied	10
2.0 RECOMMENDATIONS	12
3.0 EMI-TAD/SUBSATELLITE	14
3.1 EMI-TAD/Subsatellite Design	14
3.2 EMI-TAD/Subsatellite Costs	20
3.3 EMI-TAD/Subsatellite Mission Requirements . . .	23
3.4 Summary of EMI-TAD/Subsatellite Study.	26
4.0 SINGLE INSTRUMENT TAD	28
4.1 TAD Design	28
4.2 TAD Support Requirements	32
4.3 TAD Costs	33
5.0 SOLAR-POWERED TAD/SUBSATELLITES	34
5.1 Need for Solar-Powered TAD/Subsatellites	34
5.2 Survey of Solar-Powered Satellites	37
5.3 Recent Solar-Powered Satellite Concepts	48
6.0 ACKNOWLEDGMENTS	49
7.0 REFERENCES	50

1.0 INTRODUCTION

Very early in the shuttle science discussions it became obvious that not all scientific measurements could be made from the shuttle. One of the items that has been brought up over and over again, in the AMPS Working Group Meetings, is the fact that the shuttle presence represents a significant modification of the environment. After the first estimates of the EMI generation by the shuttle's systems, it became obvious that ELF/VLF/HF receivers and magnetometers could not be operated on the shuttle without significant background problems. The shuttle magnetic field also presents problems for the thermal plasma measurements. Because of these and other problems, a great interest was shown in defining a vehicle (TAD/subsatellite) which could be used as an experiment platform for the test flights to map the EMI from the shuttle and which could also be used during the AMPS science flights. An interest was also shown in generating ideas on a range of instrument platforms of varying capabilities. This study examines both with emphasis on the EMI test vehicle, the experiments for it, and the operational support requirements of TAD/subsatellites. TAD stands for Throw Away Detector and is envisioned as a simple instrument package for supporting specific experiments.

1.1 Overview of Instruments for TAD/subsatellites. We have reviewed the IFRD's (Instrument Functional Requirements Documents) plus the notes from the bi-monthly AMPS meetings and have extracted from these sources a list of experiments which could be included as TAD/subsatellite payloads. This resulted in a list of about twenty distinct

TABLE 1
TAD/SUBSATELLITE EXPERIMENT GROUPINGS[#]

1. SHUTTLE-ENVIRONMENT SENSITIVE EXPERIMENTS

AC/DC Electric and Magnetic Fields (14, 15, 39)

ELF/VLF/HF Waves (15, 25)

Low Energy Neutral and Charged Particles (9, 10, 16, 50^{*}, 58, 60, C, D)

Neutral and Ion Drifts (24, 38)

2. SHUTTLE-ENVIRONMENT DIAGNOSTIC EXPERIMENTS

AC/DC Electric and Magnetic Fields (14, 15, 39)

ELF/VLF/HF Waves (15, 25)

Low Energy Neutral and Charged Particles (9, 10, 16, 50^{*}, 58, 59, 60, C, D)

Sounder Transponders (11, 22)

Neutral and Ion Drifts (24, 38)

Contaminants (A)[†]

3. PARTICLE-ACCELERATOR SYSTEM DIAGNOSTIC EXPERIMENTS^{**}

AC/DC Electric and Magnetic Fields (14, 15, 39)

ELF/VLF/HF Waves (15, 25)

Low Energy Neutral and Charged Particles (9, 10, 16, 41[†], 42[†], 50^{*}, 58, 59, 60)

Neutral and Ion Drifts (24, 38)

TABLE 1 (cont.)

(3.) PARTICLE ACCELERATOR SYSTEM DIAGNOSTIC EXPERIMENTS **

Energetic Particles (53, 57)

X-rays (B)

The numbers in the brackets correspond to the experiment numbers from the IFRD package distributed in April 1975.

* Subsatellite compatible experiments measuring the same particles but with reduced geometric factors, telemetry requirements, weight, etc.

† Includes experiments which could be boom mounted on shuttle and others which could be used to monitor TAD/subsatellite potential and control it.

** While many of these experiments are similar to those in the other groups, they will be modified to be used in the beams.

+ For instruments referenced by capital letters, see Table 2.

TABLE 2
INSTRUMENTS FOR TAD/SUBSATELLITES

IFRD Number	Experiment Name	Description of Measurement Made
9	Photoelectron/Secondary Electron Spectrometer	Electrons $\sim 1 < E < 500$ ev. Measurement contaminated by large magnetic fields, large photoemissive surfaces, large physical bodies blocking particle trajectories, and high ambient gas density.
10	Neutral Mass Spectrometer	Number densities of neutral atmospheric gasses. Contaminated by effluents from shuttle and turbulence generated by shuttle. Needs unobstructed 2π field-of-view parallel to velocity vector.
11	Radio Frequency Sounder	Measure plasma propagation properties. Receiving antenna must be distant from the shuttle. Receivers are EMI sensitive.
14	DC Electric Field	Measures E , dE/dt and dE/ds of naturally occurring and artificially generated fields. Contaminated by low frequency EMI, plasma turbulence caused by shuttle and sheath potentials.
15*	Triaxial Fluxgate	B , dB/dt , dB/ds . Used for ULF hydro-magnetic wave propagation measurements. Contaminated by and measures shuttle ULF noise generation. EMI sensitive. Duplicated in 39 below.
16	Langmuir Probe	Measures thermal electron temperature, density and plasma potential. Contaminated by and measures environmental modifications caused by the shuttle. Sensitive to large B fields and surface contamination.
22	Doppler Tracking Bistatic Sounder	Measures electron density distribution in shuttle wake. Requires subsatellite borne transponder and antenna. Similar to 11.

TABLE 2 (cont.)

IFRD	Experiment	Description of Measurement Made
Number	Name	
24	Neutral Temperature and Drift Spectrometer	Measures temperature and flows of neutral atmospheric constituents. Contaminated by effluents and turbulence generated by shuttle. Requires unobstructed view along vehicle velocity vector.
25	ELF/VLF Receiver	Measures magnetic and electric field components of electrostatic and electromagnetic waves from 100 Hz to 30 kHz. Very sensitive to EMI, both conducted and radiated, in the 10 Hz to 200 kHz range.
38	Ion Drift Detector	Measures thermal ion flows. Sensitive to plasma turbulence, effluents, and electric fields generated by shuttle. Requires unobstructed view along vehicle velocity vector.
39*	Vector Magnetometers	Measures B , dB/dt , dB/ds , vehicle attitude and magnetospheric currents. Contaminated by magnetic field of shuttle.
41	Beam Diagnostics II	Measures beam current density, particle energies and beam plasma potential. Contaminated by shuttle magnetic fields, effluents, potential variation and plasma turbulence. May be useful to make some observations from a separable platform using these instruments.
42	Beam Diagnostics III	Measures dB/dt , E and plasma potential in beam. Contaminants as in 41 above. Measurements along beam may require separable platform.
50	Medium Energy Electron Detector	Measures electrons $10 \text{ eV} < E < 50 \text{ keV}$. Subsatellite version is similar. Provides remote diagnostic measurements. Low energy measurements contaminated by shuttle magnetic fields and restricted view angles.

TABLE 2 (cont.)

IFRD Number	Experiment Name	Description of Measurement Made
57	Energetic Ion Detector	Measures ions 20 keV-10MeV. For remote observations during accelerator experiments, plasma seeding and tracer experiments. Low temperature operation required.
58	Energetic Electron Detectors	Measures electrons 15 keV-3MeV. For remote observations during accelerator experiments and plasma seeding experiments.
59	Medium Energy Ion Mass Analyzer	Measures ions 10 eV-30 keV. Contaminated by shuttle magnetic field at very low energies and by shuttle effluents. For remote observations as in 57 above.
60	Ion Mass and Distribution Analyzer	Measures temperatures, densities and flow velocities of thermal ions in mass range from 1-64 AMU. Contaminated by shuttle magnetic field, effluents, plasma turbulence, and potential.
Others		Description of Measurement Made
Number	Name	
A	Quartz crystal Microbalance	Measures mass accretion rate on surface from outgassed contaminants, thruster effluents and other vaporized expendables from shuttle. Should be used to make measurements in the near shuttle environment.
B	X-Ray Detectors	Measures x-rays generated by interaction of the accelerator beams and atmosphere. Requires remote platform to make measurement of flux directed away from the shuttle.
C	Ion Guages	Measures total atmospheric density. Requires unobstructed field of view which is held on or scans through vehicle velocity vector direction. Contaminated by plasma turbulence and effluents.

TABLE 2 (cont.)

Others

Number Name

Description of Measurement Made

D

Accelerometers

Measures atmospheric density and vehicle accelerations. Contaminated by motions of masses aboard the shuttle. Requires vehicle of simple, clean shape for drag analysis. Can be used to determine effects of shuttle-induced turbulence on nearby subsatellites during low altitude operations.

experiment packages (or groups of packages). The different experiment packages have been regrouped into categories. The basic categories are: (1) Shuttle-environment sensitive experiments (primarily low energy particles and fields experiments), (2) Shuttle environment diagnostic experiments, (3) Particle accelerator system diagnostic experiments (will have direct exposure to the particle beams), (4) Special experiment-peculiar groupings. The first three of these groupings are listed in Table 1. The fourth group cannot be listed in detail without referring to specific experiments. All the experiment packages defined for subsatellites in the IFRD's plus some not listed there, are candidates for the fourth group. Table 2 lists the IFRD number, experiment name, and the type of measurement made for reference.

It is obvious that some of the experiment packages defined in the IFRD's for inclusion on a subsatellite will have to be scaled down in weight, telemetry requirements and power if they are to be used in a TAD/subsatellite (depending on the capabilities of the TAD/subsatellite chosen). In some cases, this can be done by reducing the number of duplicate instruments in instrument arrays. It is also obvious from Table 1 that there is a large overlap between the experiment packages in each group. This is to be expected since most of these experiments measure very basic physical parameters which are influenced by even slight environmental modifications and which are required in order to understand what is happening. Not all of these measurements need be made simultaneously for every situation. In order to get an idea of the maximum TAD/subsatellite support necessary for these experiments, we show in Table 3

TABLE 3

NOMINAL SUPPORT REQUIREMENTS FOR THE EXPERIMENT GROUPS

Group (from Tab. 2)	Total Weight (kg)	Power (watts)	Telemetry (kbps)	Booms Req'd.* (number)	Stabilization [#]	Attitude control (deg.)
1	80	155	68	12-14	Spin, 2-axis, 3-axis	0.01-5.0°
2	123	160	86	12-16	Spin, 2-axis, 3-axis	0.01-5.8°
3	110	160	72	10-14	Spin, 2-axis, 3-axis	0.01-5.0°

* Number of booms required is determined by whether more than one experiment can use the same boom.

Stabilization requirements were: Spin stabilized (very slow to moderate spin rates, 0.2° - 180°/sec), 3-axis stabilized with preferred orientation relative to the shuttle, 2-axis stabilized with spin axis in preferred direction and movable, and 3-axis stabilized with a scanning platform.

the totals for weight, power and telemetry. These numbers have had duplications among the instruments removed.

The main point to be realized from Table 3 is that it is impossible to provide the support requirements for all the experiment packages in a group with a single TAD/subsatellite. The large number of booms, high weight, conflicting stabilization requirements and the demanding telemetry requirements (note that the broadband requirements must be added) preclude flight of all experiments on a single vehicle. A vehicle can be designed which could support a subgroup of these experiments and which is flexible enough to support a different subgroup from one shuttle flight to the next. The AE satellite is one such vehicle, but has more capability than is required for many shuttle experiments and tests.

1.2 Items to be Studied. For particular shuttle flights it is expected that subgroups of experiments will be accommodated on a TAD/subsatellite for supporting a particular experiment or a limited fraction of an experiment. More than one TAD/subsatellite will be usually required for a shuttle flight if the proper measurements are to be made. The number of vehicles required will be determined by the complexity and number of different experiments which will be attempted on a given flight. From the point of view of supporting experiments with TAD/subsatellites, it is obvious that the experiments to be done on a given shuttle flight must be carefully coordinated. Efficient use of the TAD/subsatellites requires that experiments performed have similar or at the very least non-conflicting support requirements.

We have used the IFRD's as guidelines plus our own experience with satellite and rocket experiments to put bounds on the weight, power and TTC requirements of some of the experiment packages. We have then selected a subset of experiment packages from a group and used them to size a particular TAD/subsatellite support system. The primary goal was to define a vehicle or vehicles which could support experiments for measuring the shuttle environment during early test flights. The vehicles can also support AMPS experiments in a variety of ways.

In the sections below, we detail battery-powered TADs and a subsatellite (too large and costly to be a TAD) and we also present an array of solar-powered TAD/subsatellites. In each section we describe the shuttle/spacelab support required by each type of TAD/subsatellite and point out areas which are felt to be critical. In the next section, we make some recommendations of studies which should be done or expanded and actions to be taken.

2.0 RECOMMENDATIONS

During the course of this study, several areas were found in which we could not detail systems or support requirements because of lack of information. In some areas we were able to see that further study was required. In a few instances we have been able to recommend specific actions. We have outlined some of these items in the numbered paragraphs below. No importance is to be attached to the order of presentation.

2.1 Now that specific experiments are being chosen and assigned to shuttle flights, a serious examination of the TAD/subsatellite support required by the individual experiments should be made. Before a set has been "cast in concrete" it should be surveyed with an eye to maximizing the number of different experiments which can be supported by a single subsatellite and minimizing the number of TAD/subsatellites required during a shuttle flight. An attempt should be made to develop a time-line for the experiments which includes the operations of the TAD/subsatellite, the spatial positions it must be in, and its power requirements. The battery-operated vehicles will require careful control if they are to provide maximum support. The displays and processing of the TAD/subsatellite data must be considered in detail also for each experiment.

2.2 The experiment operation plus TAD/subsatellite usage should be examined in terms of the impact they will have on the shuttle astronauts. The existence of the TAD/subsatellite may require extra personnel for its check-out, ejection, tracking and operation. In fact, it (they) may require a dedicated astronaut.

2.3 The possibility of leaving TAD/subsatellites in orbit to support more than one AMPS mission and other shuttle missions should be considered.

2.4 The TADS (ref. section 4) should be provided as part of the spacelab experiment support system. Several should be purchased at once to fulfill the needs of the first few AMPS flights. Experimenters should be required to build their instruments to be compatible with the TADS.

2.5 Several of the battery-powered subsatellites (ref. section 3) should be built to support the more demanding experiments on the early shuttle test and AMPS flights. They should have modular support systems and experiments must be built to be compatible with these vehicle systems. The battery-powered subsatellite should be expandible into an intermediate-type satellite (see section 5) with little modification of the structure and an upgrading of the attitude control and other support systems. The EMI-TAD/subsatellite should be considered a standard experiment for AMPS as one way to provide EMI free-wave measurements.

2.6 In future studies concerning the experiments for specific shuttle flights, a better idea of the target cost that NASA is considering for the whole flight is required. Without such a guideline it is impossible to allocate resources and provide realistic options relative to the experiment, instrument, and TAD/subsatellite mix which will do the best science within allowed constraints.

3.0 EMI-TAD/SUBSATELLITE

3.1 TAD/subsatellite Design. In order to set up a plausible vehicle design we took, as a guide, the requirement to monitor the EMI environment of the shuttle early in the test flight sequence (prior to flight 8). This gave us a reasonably complex compliment of instruments around which we could design a relatively simple, but very useful, vehicle. This requirement also allows us to provide the answers to some very important questions concerning support requirements that such a vehicle would place on the shuttle.

The experiments needed to make the EMI measurements are shown in Table 4. These are not all the possible instruments (ref. Table 1) which could be used but are those we consider to be the minimum required to make unambiguous EMI measurements. The magnetometer is expected to play a dual role by providing part of the data for inertial attitude determination. The vehicle which can support these instruments can also support an array of different instruments with similar weight and power requirements. With the addition of extra power capacity, the support capability in terms of power, more instruments, and duty cycle could be considerably increased.

The vehicle system which we chose to support the experiments is shown in Table 5. This system is based upon recent rocket payloads developed at our facility and upon a range of low-cost, small satellites (some battery-powered) which have been built in the last few years for the U.S. Air Force. The telemetry system was sized to provide excess capability for expanded experiment packages for the other tests and the

Table 4

EMI-TAD/ SUBSATELLITE

	Weight (kg)	Power (watts)	Volume (cm ³)	Telemetry (bps)	Broadband* (Bandwidth)
ELF/VLF Measurements		12.5		1500	
-electronics	3.7	---	7400		ELF: IRIG-Ch. 16 30-600 Hz
-Booms (2-3 meter dipoles)	5.1				VLF: 200-30,000 Hz S/N ≥ 15 db modulation index
Electric - preamps	1.3	---	2 at 360		
- antennae	5.0				
Magnetic - antennae (2 each at 1.4 kg)	2.8	---	1600		VLF: IRIG-H 200-5000 ELF: IRIG-ch. 17 30-600 Hz
-Boom (2 meter)	1.5	---	RX200		H. F.: IRIG-ch. 18
H. F. Measurements - electronics	2.3	10.0	2700		
DC Measurement - electronics	2.7	7.5	3450	5000	
Plasma Density and Temp [#]					
a) RPA or Ion Mass Spect.	2-7 kg/unit	6.0	≤ 10000	2000	
b) Electrostatic Probe	3.5	10.0	4400	3000	
Magnetometer [#]					
- sensor	1.0		3500		
- boom (2 meter)	1.5		RX200		
- electronics	4.0	20.0 ^{**}	4800	2000	
Instrument Totals	~41.4 ⁺	~ 66	~40000 (0.04 m ³)	13,500	

Weight and power depend on type of instrument chosen. There should be two independent measurements of the plasma parameters.

* Broadband telemetry is set up for S-band, IRIG standard channels. ELF-VLF broadband channels to be time shared by electric and magnetic sections.

** Number taken from IFRDs, is probably too high.

+ Maximum weights used.

Table 5

EMI-TAD/SUBSATELLITE SUPPORT SYSTEMS

	Weight (kg estimated)	Pwr. (watts 28 VDC)	Volume (cm ³)	Telemetry (bps)
Telemetry Sys. and Command Sys. and Beacon	4.7	30W	3000	(24 kbs capacity) 1000 bps monitor functions
Batteries & Pwr. Sys.	20	(~1500 W hr. capacity)	6000 (est.)	---
Attitude Sensing	<1.0	~1.0	1000	50
Neutation Damper	1-5 [#]	---	Variable	---
Structure	24 [*]	---	---	---
Wiring	7	---	---	---
Thermal Control	1.6	---	---	---
Experiments	41.4	66	40000	13500
Totals	~ 104.7 ⁺	~97	~50000	14550

[#] Depends on satellite mass, spin rate, moments and damping time required.

^{*} Based on structure accounting for ~24% of total weight.

⁺ Maximum weights used.

AMPS science flights. The cost of the telemetry system is not large (see Table 6) and the excess capability comes essentially free. The telemetry system is based on a 5 watt S-band transmitter. This transmitter should have enough power to provide reasonable link margins for most of the shuttle altitude orbits. (There are newer transmitters available with output power capabilities of more than 8 watts with negligible difference in weight and cost if more power is desired). The telemetry system bit-rate can be sized by varying the subsystem components (such as the programmer and multiplexer). We have also included a beacon for tracking purposes. A transponder might be required to obtain the necessary position accuracy, but we have not looked at this in great detail since some information has already been generated at NASA/Marshall.

We have included a command capability in the system in order to make the instrument support flexible and to provide a means to efficiently utilize the limited lifetime of the vehicle through duty cycling its operation. It does not seem feasible to store the vehicle on the shuttle with booms extended so a commandable deployment system becomes necessary for the EMI-TAD/subsatellite. This capability is also required on the test flights since the sensitivity of the ELF/VLF/HF receivers must be changed upon command if we are to obtain usable results both near and far from the shuttle. The final vehicle system should be flexible so that the command capability can be supplied or not as the varying instrument compliments require.

Table 6
Preliminary Cost Estimates

	Cost (thousands)	
ELF/VLF Instruments*	150	(80)
H. F. Measurements*	60	(30)
DC Measurement*	50	(20)
Plasma Measurements*	150	(60)
Magnetometer	30 [#]	
Telemetry system and beacon (no command capability)	12 [#]	
Power system	10 [#]	
Attitude sensor system	2.7 [#]	

[#] Off-the-shelf hardware in 1973 dollars.

* Includes instrument development the (--) represent the reproduction costs.

We have chosen Ag-Zn batteries as the power source because they are reliable and cheap. A considerable weight and lifetime penalty is experienced by this choice, but it is considered to be the best compromise at this time for the short, simple shuttle missions such as the test flights. We feel that at least two full-shuttle orbits (one totally dedicated) are required to do any good EMI study. The power system was sized to satisfy this requirement and to provide excess capability for at least 6-7 other orbits. This gives the flexibility to repeat some measurements and to provide data in a region of space (for the early flights) which is of great scientific interest. These comments are expanded on in the section on operational requirements below.

We have assumed that the EMI-TAD will be spin stabilized and that the angular velocity will be imparted prior to launch from the shuttle. (The angular velocity could also be imparted after ejection, using spin rockets as is usually done. This possibility should be examined in terms of shuttle safety since it is relatively cheap.) The attitude-sensing instrumentation is simplified because of this and is neither costly nor heavy. A complete redundant attitude-sensing system would include the magnetometer, an earth sensor and a sun sensor. This is the system we have considered. The items in Tables 5 and 6 under attitude sensors represent the earth and sun sensor systems. A nutation damper is required to reduce nutation and is extremely cheap and simple.

The structure must be strong enough to support the vehicle during the launch environment without failure. The value chosen for this study is based on a fraction of total instrument plus vehicle systems weight

obtained by averaging over many other spacecraft. The spacecraft included in this average had launch environments much more severe than the shuttle environment. This structure, or one slightly more massive, should provide a platform suitable for many instrument mixes and may reduce or eliminate the need for structural testing because of the loading margin designed into it.

The wiring estimate is very crude and represents the wire bundle required to support an experiment complement which is about twice as complex as that shown in Table 4. The wiring bundle will be peculiar to each experiment mix, but the connector interface to the vehicle should be the same on the vehicle-system side for all vehicles. In order to reduce costs and maintain flexibility, the power and telemetry distribution interface should be fixed with the digital and housekeeping telemetry provided in fixed blocks (eg. 2000 bps digital and 5 analog lines at 1 sps as a block) and the broadband analog ports should be prewired on the vehicle-systems side. The experiments would then be allocated as many blocks as required with the broadband ports treated as special cases. The command distribution could be done in a similar manner, or logic level commands preceded by addresses could be "broadcast" to all experiments.

Most of these concepts can be satisfied by a vehicle layout as described in the recent ESRO report (AMPS-Subsatellite study, April, 1975). We can give more details and ideas about such vehicle designs at a later date but we feel that the ESRO study provides the same kind of design philosophy that we were considering.

3.2 EMI-TAD/subsatellite Costs. In Table 6 we show a breakdown of specific hardware costs as best as we can estimate them. The instrument

costs are based on actual costs of previous instruments plus an estimate of development costs required to provide instruments for these specific missions (the test flights). The vehicle systems costs that are identified represent actual costs for hardware from a rocket flown in 1974. None of these costs include cost of integration with a vehicle or vehicle systems and environmental testing. We have shown in the brackets the cost to produce copies of the instruments after the first prototype. We assume the prototype instruments will be flown.

In Table 7 we show estimates of man hours required to design, develop, build, test and support two vehicles of the type defined in Table 5. These numbers are based upon actual experience with battery-powered vehicles which were very similar to the one defined in Table 5 and which had similar experiment compliments. We have not included in the man hour estimates the time required to design and develop the hardware interface with the shuttle or the mechanisms for imparting the angular velocity for stabilization. The dollar estimate given in the summary was obtained by adding the instrument and equipment costs from Table 6 (for two sets) to the number of man years multiplied by 0.03 M/man-year and dividing the result by two ($[0.71 + 1.48] / 2 = 1.09$). This result includes overhead, but is probably a conservative estimate.

For each succeeding identical vehicle the effort for each task in Table 7 is considerably reduced or nonexistent. The major costs which recur with each identical vehicle are the cost of actual production of the items, assembly and checkout, integration, pre- and post-launch support and program management. If vehicles are produced which have

Table 7

Apportionment of effort for two vehicles[#]

	Man Hours
1. Experiment support definition	4000
2. Experiment analysis	4100
3. Program management and coordination	5800
4. Systems engineering and development	15400
5. Reliability maintenance and safety	1200
6. Vehicle hardware manufacture	33800
7. Vehicle integration	14800
8. Final assembly and checkout	3200
9. AGE/GSE	2800
10. Spares	1000
11. Refurbishment and tool maintenance	800
12. Prelaunch operational support	3400
13. Post launch support	700
14. Design review support	3700
	<hr/>
Total	94700
Equivalent Men (1920 Hr. / Man Year)	49.3

[#] No effort has been allotted for interfacing the vehicles with the shuttle other than for telemetry/command-control compatibility checks.

the same basic design but some differences in detail, instruments and support requirements, then the experiment support definition and analysis, some systems engineering, some development and new testing will probably be required but at a much reduced level from that shown in Table 7.

3.3 EMI-TAD/subsatellite Mission Requirements. We have made an examination of the mission requirements which must be met to perform the EMI study. Many of the items detailed below are in response to questions raised at MSFC/JSC and others represent questions we have raised and which need to be cleared up before a detailed vehicle design is undertaken. We feel that a minimum of two EMI-TADs are required for each test flight. One is to be considered a backup unit which can be brought back if not needed.

The EMI-TAD must be capable of being moved about the shuttle on the manipulator arm. This will be the only safe method of obtaining the very-near-shuttle measurements. The EMI-TAD will not be hardwired to the shuttle while on the manipulator arm. It will be operated as a free vehicle. Not all of the booms will be extended when near the shuttle.

The TAD should be ejected from the shuttle with small ΔV (≤ 1 m/sec), preferably from the manipulator arm. A mechanism to provide the spin can be built into the launcher or the spin can be initiated after launch if safety and ejection errors allow it. The EMI-TAD/subsatellite should have a spin rate of ~ 2 rpm with booms extended. For the near shuttle measurements (50-500 m) it will be necessary to fly the shuttle in formation with the TAD/subsatellite to reduce or cancel the separation rate of the

two vehicles. Then the shuttle ΔV can be "tuned" to obtain a moderate separation rate which will keep the TAD in "sight" for the duration of the mission.

It is preferred that these EMI studies be carried out at 300-400 km altitude (the region of maximum electron density). The inclination of the orbit should be near 28° or 56° and not in between. One flight at each inclination is best in terms of operational and scientific information return. At least one orbit from each test flight must be dedicated to the EMI study only. A second orbit would be useful and may be necessary depending on the time required to cycle through power configurations. The shuttle should be rotated very slowly through 360° in pitch and then roll while the operations related to changes in the power profile and operating equipment mix are varied to give a complete spatial and operational EMI profile. This should be done as a function of distance between the TAD and the shuttle.

It is very critical that an exact, detailed record of the operational profile and orientation of the shuttle be made during the experiment. The accuracy of the timing of the different events is very critical. This probably requires that the EMI-TAD transmit all data to the shuttle, during the test, so that it can be inserted into the shuttle data-stream along with the shuttle time-base for transmission to the ground. This requires that the shuttle be capable of providing a receiver link with the EMI-TAD/subsatellite and position and ranging information in any attitude

configuration relative to the TAD/subsatellite. The EMI-TAD/subsatellite range and angular position in shuttle coordinates is required. This must be very accurate (~1%) for distances less than 500 m. One could use stereoscopic TV tracking or possibly photographs against the star field (good only for post flight analysis). There are many other possibilities which have been discussed at the Working Group Meetings and they will not be covered here. It suffices to say that the tracking of the TAD is very important to the success of the experiment. The EMI-TAD telemetry command system must also be compatible with and capable of being received by and commanded from the shuttle, the ground stations and from either of these via the TDRS system.

The digital telemetry from the EMI-TAD/subsatellite should be processed by the computer and displayed to monitor vehicle and instrument health. The tracking outputs (for example, the readout from the stereoscopic imagers) should be processed and displayed to show the relative positions of the shuttle and TAD in shuttle-centered coordinates. The broadband wave measurements should be spectrum analyzed (analyzer to be part of shuttle support system and computer controlled) and displayed as power spectra. The power spectra should be separate for electrostatic and electromagnetic waves. The magnetometer outputs should also be analyzed in the ULF range and displayed as above. It should be possible to present these spectral displays on a single high resolution CRT, along with a display of the relative vehicle positions and the magnetic field. Another display will be needed to present the processed plasma data

(plasma density, temperature, flows, dn/dt , etc.) plus the power profile of the shuttle. These displays must be continuously monitored during the EMI tests so that unexpected outputs can be checked to see if they are shuttle related and repeatable. It would also be very useful to have these CRT displays transmitted on the TV link to the ground for display to the science team. Two-way ground-to-shuttle communications between the science team and the payload specialists, during these tests, should be available.

There is no reason to limit the test-flight environmental diagnostics to measurements of EMI. There are also questions of environmental contamination and modification (because of the presence of the shuttle) which should be studied, at least in a preliminary way, prior to the first science flights. The EMI-TAD/s subsatellite instrumentation could be expanded to provide such data (eg. instruments 10, 60, A, C and D from section 1). This would give the experimenters a more realistic estimate of the contamination to be expected in their measurements and allow them to take steps to minimize the effects.

3.4 Summary of EMI-TAD/subsatellite Study. We have looked in detail at the requirements for an instrument package which could be used on the early shuttle flights to study the EMI environment on and near the orbiter. A baseline battery-operated vehicle has been detailed which will support the instrument package and is flexible enough to support a wide range of other experiment mixes. It is felt that a simple modular structural concept such as that presented in the recent ESRO study (AMPS-Subsatellite Study, Final Rpt. by G. L. Duchossois and D. Dale, April 1975) for the TAP

and ACSAT is the correct vehicle design philosophy. We have examined the effort to build two EMI-TAD /subsatellites as defined above and estimate that the cost will be in excess of 1.0 M each. The per unit cost will drop considerably as the number increases since the systems engineering, development, etc., costs will be highest for the first vehicle. The integration, testing and manufacture should also be reduced as the main vehicle systems are reproduced on successive vehicles. The study presumed that the prototype vehicles would be flown and that the vehicles are designed to reduce testing to a minimum. The EMI tests require constant monitoring of computer-controlled displays, continuous reception of the EMI-TAD/subsatellite transmissions, accurate tracking, and precise timing of shuttle events. These support requirements make sizable demands on the shuttle systems and the astronauts.

4.0 SINGLE INSTRUMENT TAD

In this section we outline some ideas for a simple ejectable instrument package. It was presumed that each instrument package would support a single or very limited number of experiments for a few orbits (we chose ten orbits for this study) of a shuttle flight. We assumed that the instruments would be built by the experimenter and interfaced with the TAD by him. What results is a true Throw Away Detector system.

4.1 TAD Design. Likely candidates for such a TAD are simple instruments such as a magnetometer or particle spectrometers with magnetometers for magnetic attitude (reference - Minutes of $E_{\parallel} B$ rocket 21.035A; May 1975, B. Bernstein, P. Investigator). The weight and power requirements of such a TAD would vary with detector/magnetometer design, telemetry rate and transmitter power requirements.

The TAD-B (ref. Table 8) assumed a single axis magnetometer for attitude relative to B . This magnetometer would not be of the sensitive experimental-instrument quality of that utilized in TAD-A (ref. Table 8). It is seen that little weight and power would be added to TAD-B by making the magnetometer a precise instrument, though the cost would be increased by essentially the cost of the precision magnetometer. To make magnetospheric current measurements it might pay to provide both a triaxial fluxgate and an alkali-vapor magnetometer for inter-comparison. This would not change the support systems much (slightly larger battery) but the cost of the TAD would be increased by the cost of the extra instrument. While these instruments obviously do not exhaust all possibilities, they are representative of the kinds of packages many experimenters are considering for supporting particular experiments.

TABLE 8TAD Parameters

Component	Weight (kg, est.)	Volume (cm ³ , est.)	Power (watts at 28 VDC, est.)	Telemetry (Kbps, est.)
TAD-A				
Three axis magneto- meter system	6.0	8500	4*	3.0
boom - if necessary	1.5	RX200	---	---
Telemetry and trans- mitter# system	4.7	3000	30	---
Batteries	7.0	2100	---	---
Totals	<u>19.2</u>	<u>~ 13600</u>	<u>34</u>	<u>3.0</u>
TAD-B				
Spectrometer system	5.0	6000	5	10.0
magnetometer attitude system--one axis	4.0	5000	4*	1.0
boom - if necessary	1.5	RX2000	---	---
Telemetry and trans- mitter system	4.7	3000	30	---
Batteries	8.0	2100	---	---
Totals	<u>23.2</u>	<u>16100</u>	<u>39</u>	<u>11.0</u>

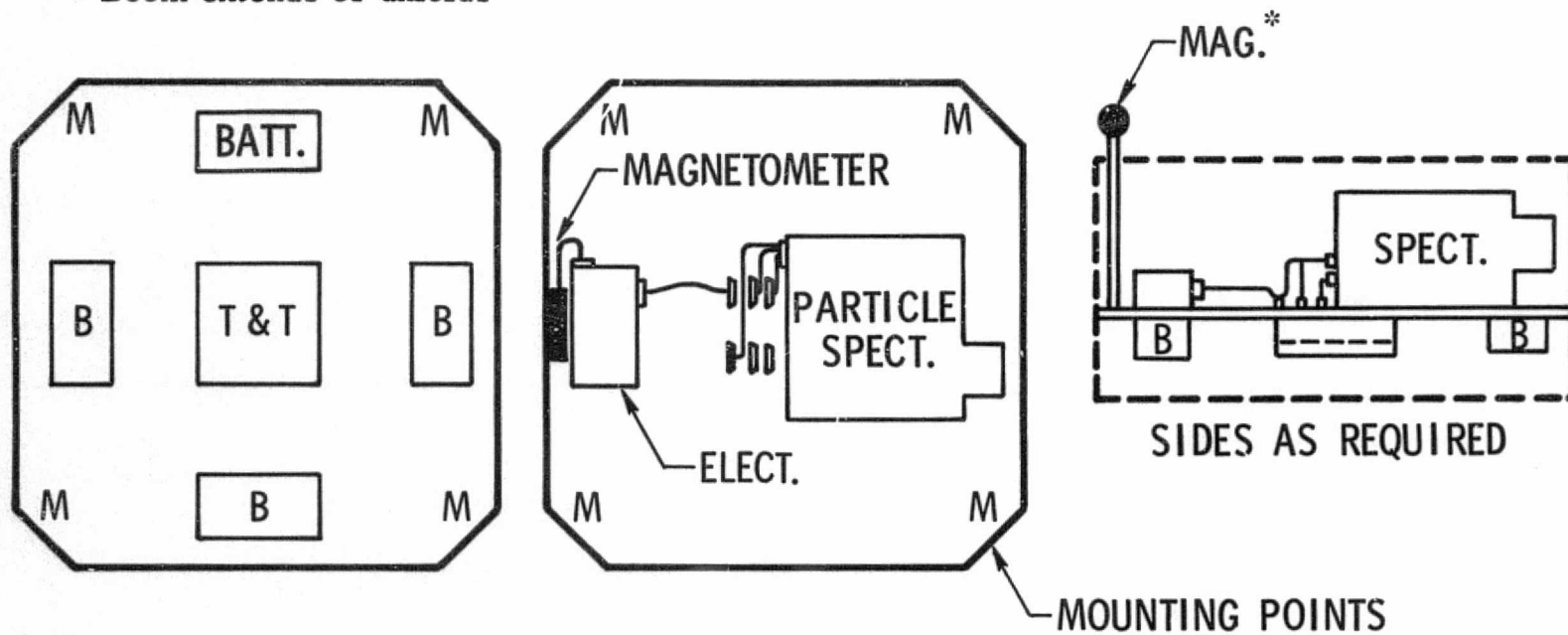
*Range of estimates from IFRDs was 4-20 watts.

#Same telemetry and transmitter system as that described in Section 3.

Two alternative approaches can be taken in the production of these TADs. One would be to let each experimenter build his own, limited only by the interface specifications of the shuttle. The second, and to us the most cost effective, alternative is to have the spacelab facility provide the TADs and let the experimenter build his instrument to meet the TAD interface specifications. Thus, the TAD structural design, engineering, testing and shuttle interface generation would be performed once by NASA or their TAD contractor. Several TADs could be purchased at one time to reduce costs. The resultant TAD should be a simple open structure with a modular support system. One such design would be a simple base plate with batteries and TM system mounted on one side and experiments mounted on the other (see Figure 1). The plate could be enclosed with walls or not, as required for thermal control and shuttle/launcher interface. The TAD structure should be capable of supporting about 0.015 m^3 of instruments weighing about 12-15 kg.

The TAD electrical interface should offer no or very limited support options and all experimenters would be required to build their instrument packages to the pre-existing TAD specifications. (This also allows the experimenter to build the instrument and test it well in advance without numerous interface definition meetings and changes.) The TM system support should be modular with fixed blocks of telemetry provided at each interface connector. The instrument would utilize as many ports as necessary. The telemetry bytes should be of fixed length (8 or 12 bits are reasonable) with proper timing and gating signals provided. The TAD support system should also provide the necessary attitude sensor(s)

* Boom extends or unfolds



SKETCH OF TAD-B

FIGURE 1

with limited options. The TAD would have a fixed mechanical (and electrical if necessary) interface with the shuttle. The TAD could be powered by switch closure at separation or by a separate mechanism. The latter would be preferred since this would allow the TAD to be given a final "liveness" test before ejection. It will probably be spring launched unless large ΔV s are required for some instruments (nominal velocities $<10\text{m/sec}$).

4.2 TAD Support Requirements. The launcher must be able to impart a spinning or tumbling motion to the TAD about a preferred axis. The launcher should be capable of launching a minimum of six TADs during a shuttle flight and should be able to launch in any direction relative to the shuttle's orbital velocity vector. It would appear that the launcher must be gimballed or that the manipulator arm be used to either launch the TADs or orient the launcher. There will also be a requirement to launch several TADs in succession (launching at a rate up to one every 30 seconds) in order to obtain a preferred spatial distribution of TADs/instruments relative to the shuttle and/or each other.

The tracking of the TADs is very critical and demanding. For some experiments such as the echo or field-line-tracing experiments, the knowledge of the TAD position is very critical. We have commented on some means of tracking subsatellites above and will not discuss it further here. It is sufficient to point out that if their positions are not accurately known relative to the shuttle and to each other, then it will be difficult, if not impossible, to make use of their measurements. Depending on the method finally chosen for tracking the TADs, the structure or the support

systems may have to be different than the simple design we have been considering.

The TAD telemetry must be received by the shuttle. The instrument output must be processed by the computer in a pre-determined manner with simple diagnostic information displayed for the payload specialist. The computer must monitor the TADs "state of health" and the battery state of charge and will display alerts if problems are sensed. Intermittent display of the relative positions of the shuttle and TAD(s) along with other information such as the mapping of the magnetic field lines through their positions, will be required for specific experiments. This area of spacelab support of the TADs during experiments cannot be detailed without considering specific experiments.

4.2 TAD Costs. Since we have almost no experience with such small free flying instrument packages we will not attempt to provide a detailed cost estimate. A rough estimate can be obtained from Figure 6 in the next section. Some accurate cost figures should be available for a similar type of package which is being considered for a rocket flight (reference NASA rocket 21.035 A, B. Bernstein, Prime Investigator). The primary design and support effort is being provided by NASA and the numbers should be easily available to MSFC. The instrument costs should be comparable to those listed in the IFRDs and in section 3 above.

5.0 SOLAR POWERED TAD/SUBSATELLITES

5.1 Need for Solar-Powered TAD/subsatellites. Utilization of TADs/subsatellites for support of AMPS experiments is required by all working groups. The level of complexity required of these TAD subsatellites is related to the kind of experiments they are to support. For example, the TADs for supporting an echo experiment could be quite simple, essentially of the type described in section 4 above. Such TADs, if distributed properly in space relative to the shuttle, give the experimenter a 'one shot' chance to run through a series of beam injections while looking for the return from the opposite hemisphere. The experiment is 'one shot' only if the TADs are simply ejected and no attempt is made to match their motion with the shuttle. Given the greater complexity of relative geometries between the TADs, the shuttle and the return-beam position over that which occurs for a rocket shot, it would be best to provide many chances to perform the experiment by a judicious choice of TAD distribution and maximization of the time spent by the TADs in the best positions relative to the shuttle. In such a case, the TAD must survive for many orbits or even days. Such constraints must be considered when sizing the power system for the TADs.

Early in the AMPS missions much must be learned about the accelerator facility itself. This requires a more sophisticated experiment platform of the type discussed in section 3. For this, an array of specialized experiments is required which can survive direct impingement of the beam while making the measurements and also provide useful diagnostics

outside the beam and at large distances from the shuttle. This can be done with a passive, battery-powered platform if the shuttle is 'flown' in formation with it to obtain the proper relative positions, or if the platform is injected into an orbit which slowly recedes from the shuttle while the accelerators are run through their paces. The shuttle can then be repositioned relative to the platform for another series of experiments if the time and effort required do not outweigh the experimental return or the cost of a second platform. Such an experiment platform must itself be able to withstand the direct impingement of the beam and must be designed so that the surface of the vehicle is not charged by the beam current to unreasonable values. The tolerance to charging will be determined by the experimental measurements, but should not be more than a few percent of the beam energy at most. The time-lining of the experiments and tests for these early shuttle flights is also extremely critical (ref. section 2). This is primarily due to the rapidly changing spatial characteristics of the ionosphere and magnetic geometry at low altitudes.

One would hope to have these experimental platforms support a variety of experiments on any given AMPS flight. This is especially true for the more complicated TAD/subsatellite platforms. The cost of these items is too high to consider them as expendable after tens of minutes, or even a few hours, of experiment operation. Some of these platforms will have costs which are an appreciable fraction of, or almost equal to, the projected launch costs (ref. section 3 and fig. 6 of this report). When it comes to the maneuverable AE type subsatellite, one must consider recovery of the vehicle to replenish expendables for a later

mission or plan to leave it in orbit and rendezvous with it on a later mission. This latter procedure may also be useful for better utilization of subsatellites which are much less complex and costly than the AE type vehicle, but still an appreciable expense. This may be quite feasible since initial indications are that many AMPS missions will be flown in essentially the same orbits. (It should also be noted that some of the AMPS subsatellite instrumentation can also be used by other shuttle experiment programs, especially the energetic particle, optical spectrometers, imaging systems and x-ray detector systems.) Recovery of the intermediate subsatellites should be considered, at least in so far as to indicate the mission-time and costs versus subsatellite costs and the overall benefits of using the experiments over again. If there is a dollar limit at which it becomes feasible to recover the vehicles for re-use, then those vehicles need to have their support systems sized for the duration of the shuttle flight only. This means that battery power may be acceptable even on an AE type vehicle if shuttle payload weight is not a problem.

For cases where it is feasible to rendezvous with a satellite for a later AMPS (or other shuttle) mission, for experiments which require diagnostics very remote from the shuttle orbit, and for the longer shuttle missions where battery-powered TAD/subsatellites would not last for the duration of the whole mission, solar-powered TAD/subsatellites are the best choice. This is also true for the diagnostic measurements required by some of the chemical release and tracer experiments. These measurements must be taken over the long time periods which correspond to the transport times into and within the magnetosphere. These times range from many hours to tens of days depending on the specific experiment being performed and the level of substorm and other magnetospheric disturbances. Many modification experiments will also require diagnostic measurements of the environment as it relaxes to the unperturbed equilibrium state. This

could require many hours and even days after the end of the shuttle mission since, for some experiments, the shuttle itself represents a non-negligible perturbation of the medium. Because of these requirements, there is definitely a need for solar-powered TAD/subsatellites. Not all of these experiment platforms will need to be as complex as the AE type spacecraft. There are many solar-powered vehicles which have been previously built and flown, from the very small (experiments plus satellite weighs less than 20 kg) to the large and complex (ref. Adamski, 1961). To give an idea of the range of possibilities for such vehicles, we have outlined some below and list their capabilities and relative advantages. We do not consider the AE type vehicle, since it has been thoroughly discussed in the MSFC documents.

5.2 Survey of Solar-Powered Satellites. The TAD/subsatellites described are flight proven designs which were developed as low cost experiment platforms which provide different levels of experiment support. These vehicles were all designed as secondary payloads to be launched 'piggyback' on a space/weight available basis or as a combined group of experiment platforms aboard a single launch vehicle. Three of these subsatellites have been designed to interface with injection motors.

The smallest of these TAD/subsatellites is the OV5 type of vehicle (see fig. 2). These could be called solar-powered TADs. The OV5 shapes were chosen as tetrahedrons or octahedrons because they provide minimal variations in projected areas, regardless of orientation relative to the sun, and thus, yield nearly constant power output from a body-mounted solar array. The octahedral shape proved to be the most desirable from the viewpoint of dynamics, structural strength, fabrication, testing accessibility and ease of stowage. These 'TADs' were capable of supporting several experiments, such as solid state telescopes and/or magnetometers (for attitude only), with relatively low power and telemetry requirements. Table 9 shows the kind of support capabilities such a satellite of moderate size might have. Table 9 also shows the support capabilities for three other vehicles.

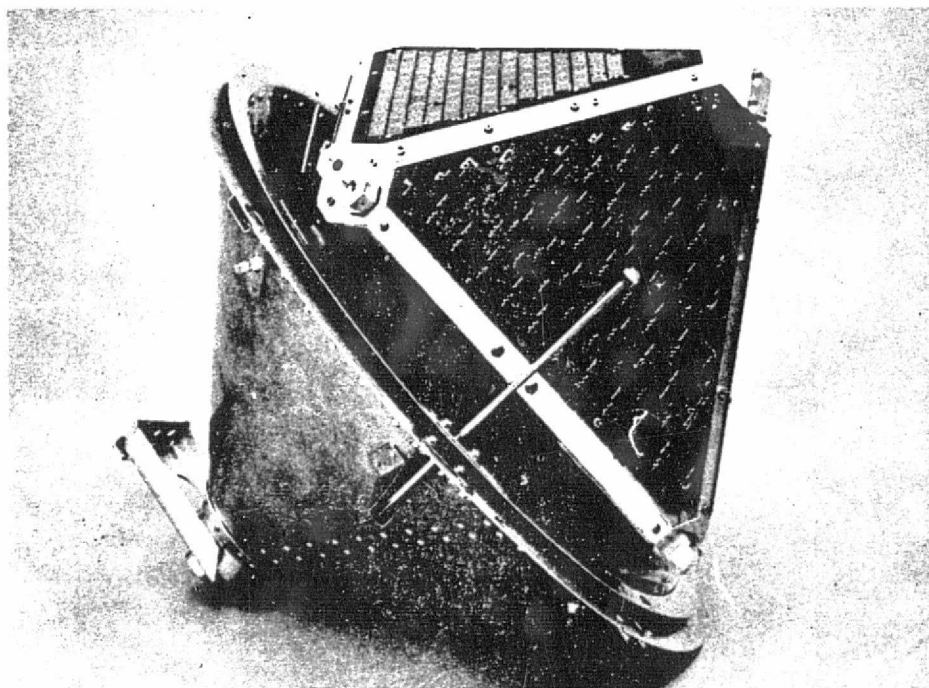
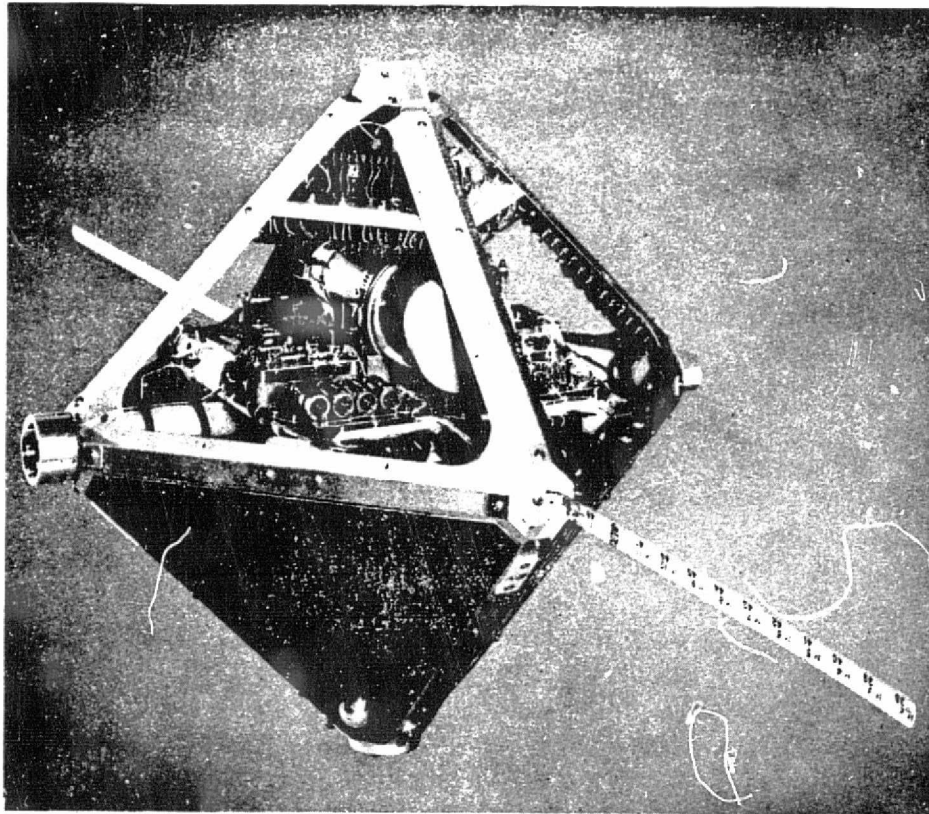


Figure 2. ORS-III with Containment Canister

Table 9

Solar Powered TAD/Subsatellite
Characteristics

GENERAL FEATURES	TAD/Subsatellite			
	OV 5 [*]	OV 3 [#]	OV 1 ⁺	S 3 ⁺⁺
Vehicle Weight (kg, no payloads)	6.2 - 9.0	54 - 82 + injection motor	59 + injection motor	97 + injection motor
Estimated Experiment Weight Capability (kg)	7.5 - 9.0	27 - 59	91	52
Experiment Power ^{##} (watts, continuous)	2 - 3, regu- lated w/25% eclipse	20 - 80	7 w/25% eclipse	≥ 20 w/25% eclipse
Volume for Experiments (cm ³)	6500	1.3 - 2.7 (x10 ⁵)	1.7 x 10 ⁵	10 ⁵
SPECIFIC FEATURES				
Electrical Power Sys.				
Total Weight (kg)	3.3 max.	23 nominal	14 nominal	≤ 19
Total Power ^{##} (watts, cont.)	5-6 max.	30 - 140 max.	100 max. w/ extra panels	>35 w/ 25% eclipse
Telemetry System				
Radiated Power (watts)	0.1 - 1.0	2 nominal	8	8.5
Weight (total)	2 - 5	4 - 7	2 - 16	18.4
Bit Rate (kbps, digital) ^{**}	.26 - 2.0	≥ 1	2 - 5	16
Storage (M bits)	0 - 2 x 10 ⁻³	≥ 10	72 max.	200 max.
	L.C. storage	----- tape storage -----		
Broadband Capability	no	yes	yes	yes
Stabilization System				
Nominal weight (kg, spin stabilized)	0.05 - 0.1	6 - 16	13	15.3

Table 9 (continued)

SPECIFIC FEATURES	OV 5*	OV 3 [#]	OV 1 ⁺	S 3 ⁺⁺
Possibilities				
Spin Stabilized	yes	yes	yes	yes
3-axis Stabilized	no	yes	no	yes
Magnetic Stabilization	yes	yes	possible	no
Gravity Gradient	no	yes	yes	no
OTHER FEATURES				
Tracking Beacon	---	yes	yes	yes
Command System (weight, kg)	0.8 - 1.0	in telemetry sys.	in telemetry sys.	in telemetry sys.
Number of commands †	up to 21	≥15	~ 30	126

* For ORS III vehicle with 28 cm side length. Vehicles with greater capabilities, larger volumes and even 3-axis stabilization have been designed, but not flown.

Four vehicles have been flown. A wide range of support capabilities are available in terms of volume, weight, etc. The numbers used are nominal ranges.

+ Ten OV1 type vehicles have been flown. The numbers represent nominal values for this type of vehicle.

++ Three S3 type vehicles have been constructed for low altitude (<6000km) orbits and have their own apogee motors. The numbers represent the latest design modified for a scout launch.

The power available can be increased by 20 - 50% if latest reliable solar cell technology is used. Cost per watt is approximately the same for new and old cells.

** The bit rate on the OV5, OV3 and OV1 systems can be increased if newer hardware is utilized. The OV3 and OV1 should be closer to the S3 values.

† Number of commands is highly variable. The numbers are based on relay closures. Use of magnitude commands increases capability by large factors.

Since the OV5 is solar-powered, it can be run continuously with little or no monitoring by the shuttle. This is useful since it reduces the workload of the astronauts and/or ground station personnel by relieving them of TAD systems cycling and commanding. The OV5 type TAD would continue to transmit throughout the whole mission and could be recorded or not as was necessary. For most battery-powered vehicles, the experiments and transmitter would have to be commanded on and off to conserve power in order to support the total seven-day mission. As long as the continuous power capability of the TAD/subsatellite is greater than or equal to the sum of experiment plus vehicle systems requirements, then the vehicle never needs to be powered down. Given the tight time limitations during a shuttle mission and the critical nature of the diagnostic measurements, to have the TAD/subsatellite always on and operating will save astronaut effort and reduce the possibility of losing crucial measurements.

The OV3 vehicle (see Fig.3) is similar to many NASA vehicles. The barrel shape is best utilized as a spin stabilized platform although, as Table 9 shows, designs exist for other modes of stabilization. The OV3 offers a relatively large experiment volume and moderate telemetry and power capability. Designs which include auxiliary solar panels for increased power capability are also available. The mechanical design is simple and has possibilities for growth potential. The design separates the experiments physically from the spacecraft support systems. This makes it easy to use a modular support system without redesigning the vehicle frame for each different mission.

The OV1 and S3 vehicles (ref. Figures 4 and 5 respectively) are different concepts of experiment platforms. The OV1 is designed primarily for heavy experiments with relatively large volume, but with limited power requirements. The power system can be upgraded with the addition of solar panels distributed about the experiment bay. This spacecraft had a propulsion module which was designed to mate with it. This gives this particular vehicle great flexibility in attaining orbits different from the shuttle orbit.

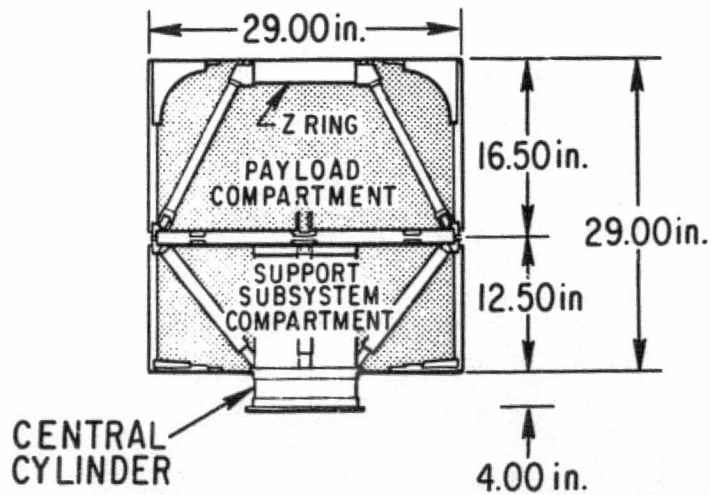
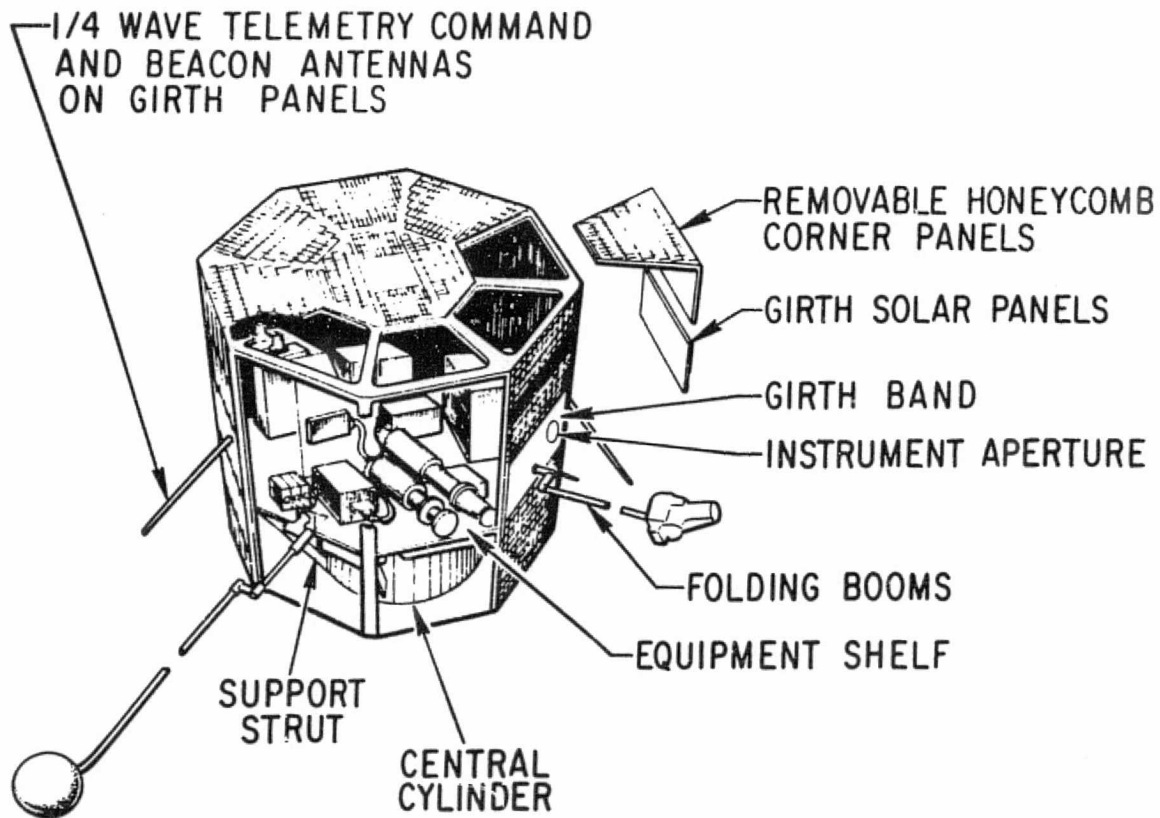


Figure 3. OV3 Spacecraft Basic Configuration

The S3 vehicle is a recently developed secondary spacecraft. As with the other spacecraft described in this report, the design requirements were for a rugged, simple vehicle which utilized off-the-shelf electrical hardware and over-designed mechanical structures which would require minimal testing. The hardware and software used in the S3 are of recent design. The spacecraft supports a relatively large set of experiments with moderate power and weight requirements. In experiment support, it represents a compromise between the OV3 and the OV1 type vehicles. The original satellites contained their own solid fuel apogee motors while the most recent design is compatible with a scout launch vehicle. A vehicle with similar experiment support systems, but cylindrical geometry, has also been flown (called P72-1).

All of these basic spacecraft have body-mounted solar panels for simplicity of design and stowage. Additional power can be made available by adding solar panels on the OV1, OV3 and S3 vehicles, but this would increase the complexity, cost, and handling problems. The power numbers shown in Table 9 assume 10% conversion efficiency for the solar panels. The newer solar cells which have 12-15% efficiency can give increased power from the same array area at about the same cost per watt.

The OV5 utilized a simple spring-ejection mechanism which is quite suitable for the shuttle. The other vehicles used a standard marmon clamp system to mate the spacecraft with the launch vehicle. The larger vehicles have their own spin rockets for spin stabilization.

The ejection systems were designed to have minimal impact on the launch vehicle operations and were found to be very reliable. Since all of these vehicles were secondary payloads, they could not interfere or endanger the rest of the payloads. Thus, severe safety margins have been built into the ejection systems, mating hardware and spacecraft structures.

These vehicles are intermediate in complexity between the TADs we have described above and an AE type vehicle and should be suitable

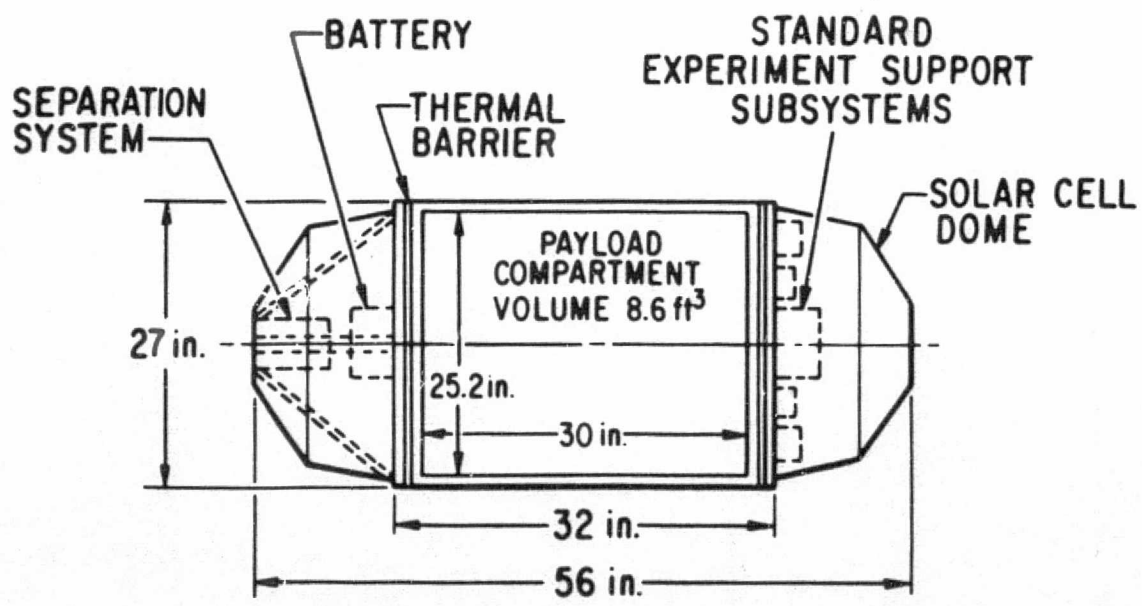
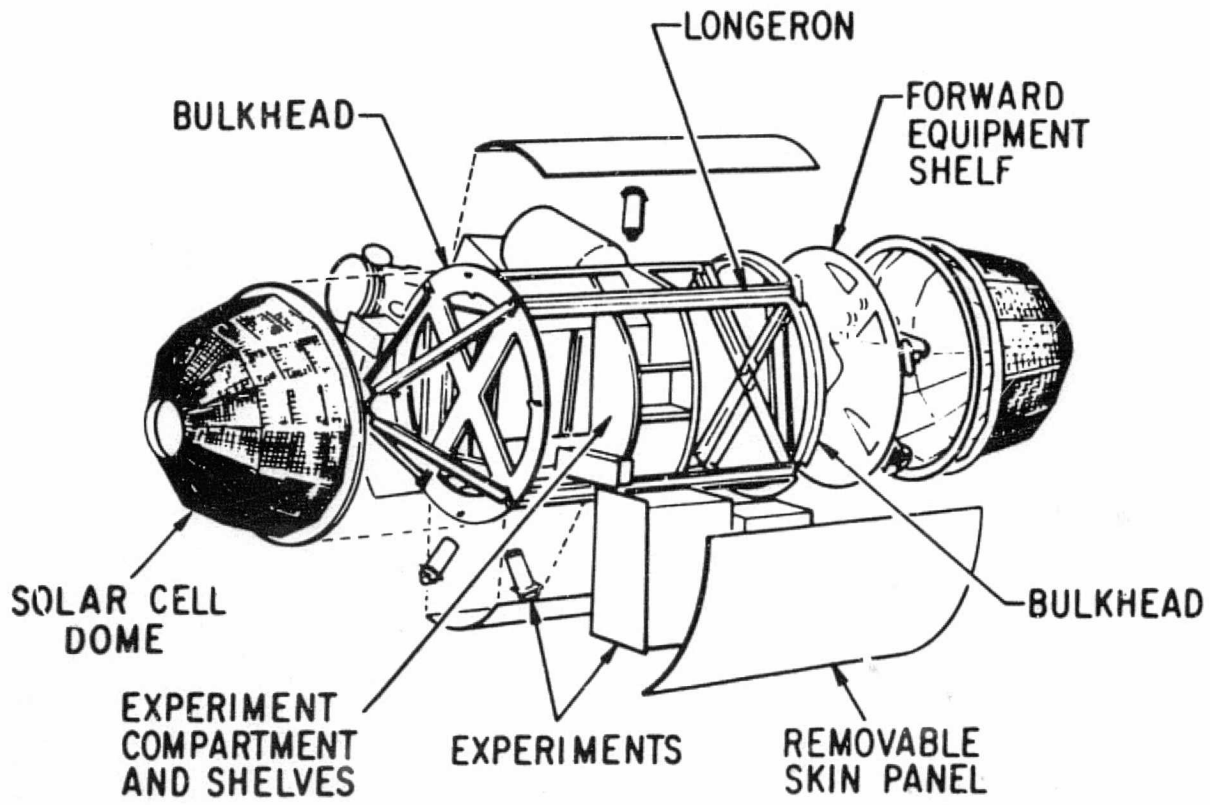


Figure 4. OV1 Spacecraft Basic Configuration

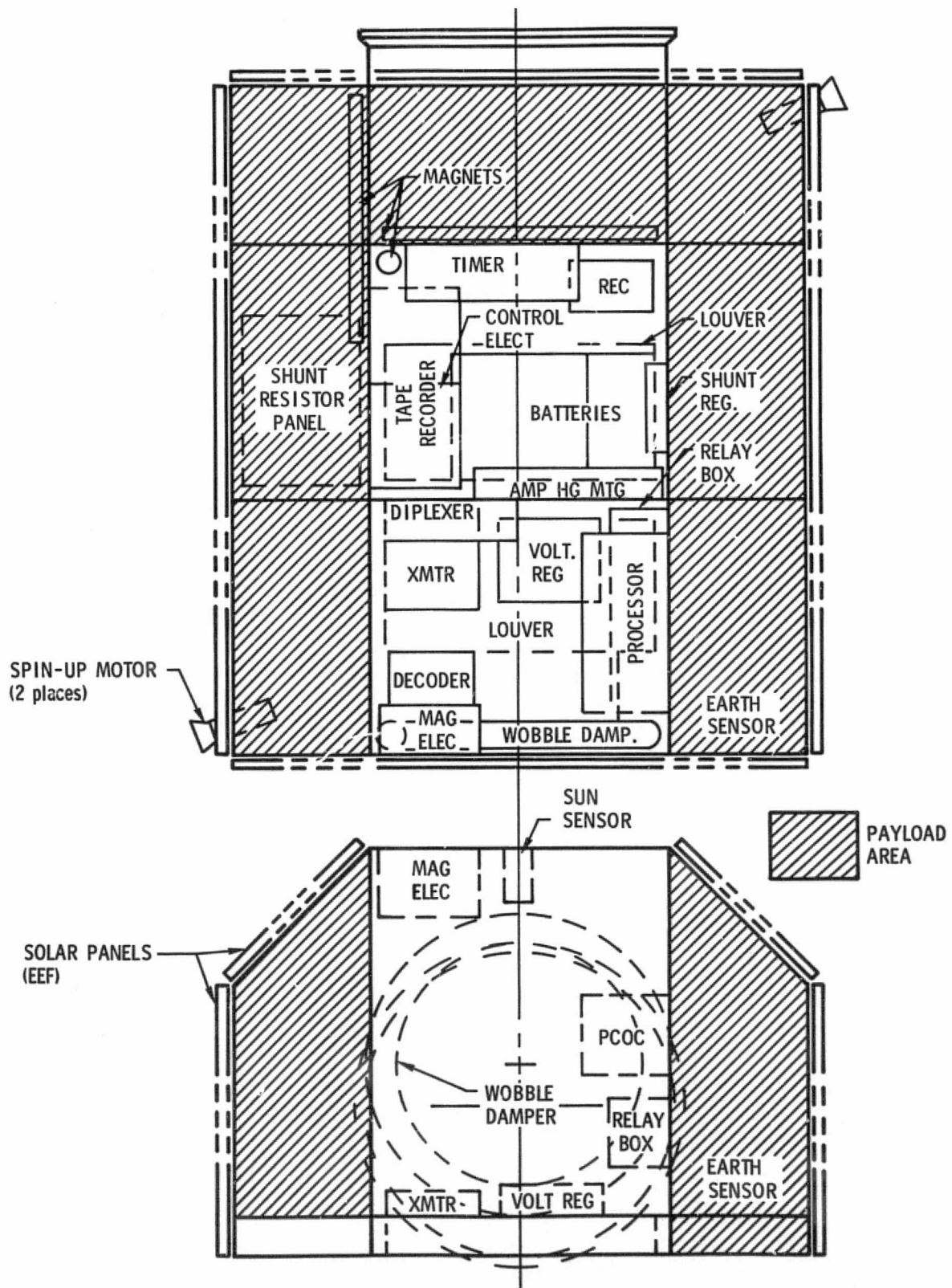


Figure 5. S3 Spacecraft Basic Configuration

for a wide range of shuttle missions which do not require a maneuverable subsatellite. In Figure 6 we show cost estimates of solar-powered vehicles based on actual costs at the time of manufacture, modified by the inflation factors to represent 1974-75 dollars. This figure has been modified from that shown in the fifth monthly report. A more accurate estimate of the inflation factors has resulted in a lower cost estimate. The new figure also includes a more accurate picture of the S3 type vehicles by showing the range of weights and different costs per vehicle. The hardware represented by the curve includes the structure, telemetry, command, electrical power, thermal control, stabilization, propulsion systems (where applicable) and the testing of these components. Experiment weights and costs are not reflected. Launch vehicle and launch vehicle integration costs plus flight support and mission peculiar software costs are not included. Aerospace ground equipment (AGE) and experiment integration costs are estimates only since these vary from mission to mission. The X marks our cost estimate of the EMI-TAD/subsatellite (ref. section 3) which was done independently. The heavy cross (+) represents the recent range for S3 type vehicles. From this graph, we would predict the cost of a TAD, which supports seven kilograms of experiments, at about \$175-225 (depends on complexity of support systems). The upper level of the band in Figure 6 would include apogee motors or special design modifications. The cost of 3-axis stabilized vehicles is significantly greater (factors of 2 or more) than the cost of a spin-stabilized vehicle. (eg. the cost of a 3-axis stabilized vehicle weighing about 550 kg would be of the order of \$12M.) The rapid increase in all spacecraft related costs in the last few years makes it nearly impossible to give reliable estimates of the costs of a given vehicle for the 1979-1980 time-frame. The costs shown in Figure 6 are intended as 'ball park' figures only. The actual costs will reflect the types of cost management, testing requirements, and quality assurance control systems required, plus additional hardware complexity that the actual spacecraft might have. With cost escalating rapidly, we think there is definitely a place for vehicles of intermediate complexity and solar-powered spacecraft in the AMPS missions.

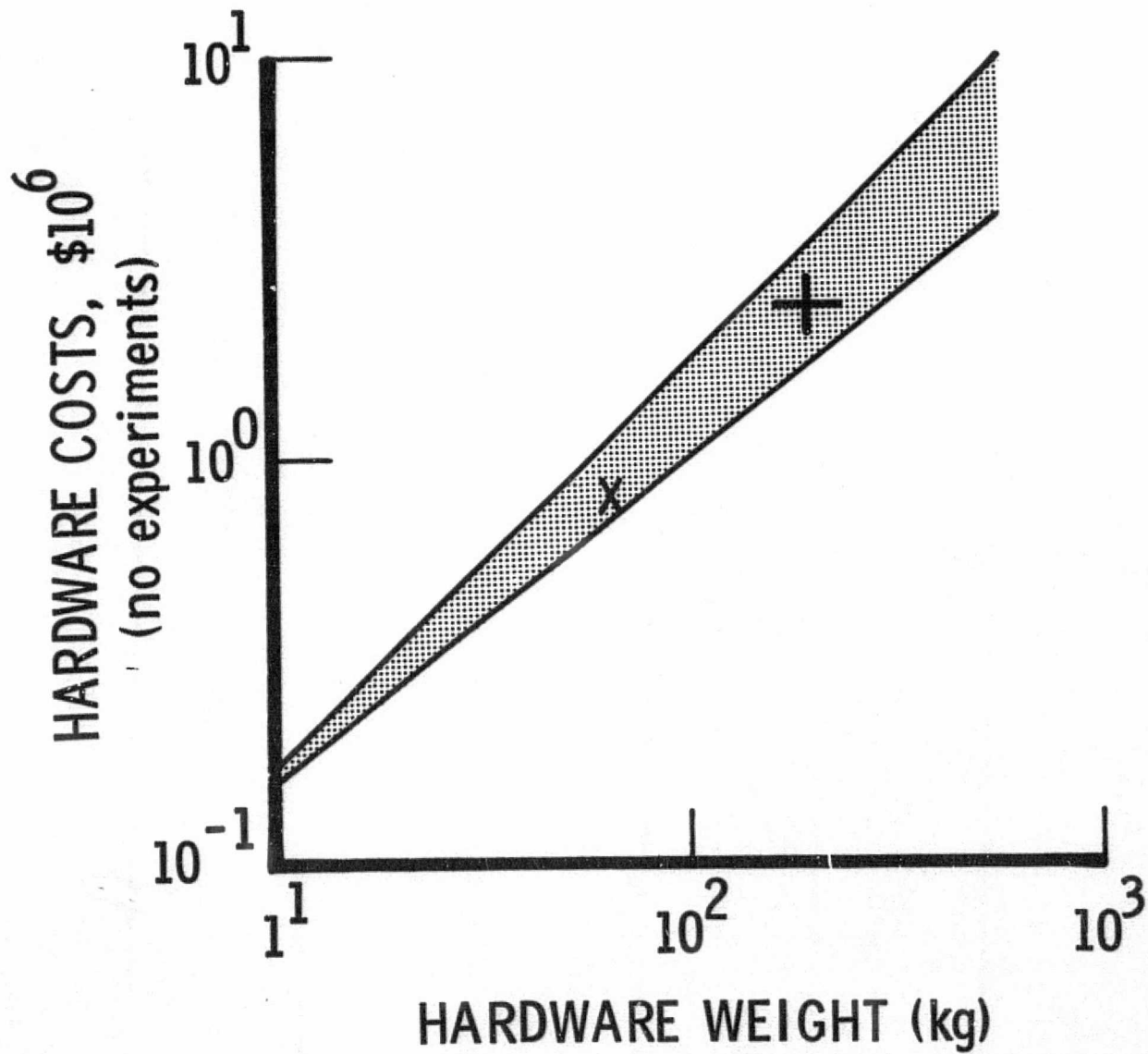


Figure 6. Estimated spacecraft hardware costs versus spacecraft weight (no payloads).

5.3 Recent Solar-Powered Satellite Concepts. More recently, studies (eg. references 2 and 3 and the Goddard Modular Satellite Study) have been undertaken to detail a state-of-the-art satellite for use with the shuttle. The objective of the Air Force study, as an example, was to design a standard satellite of great flexibility which would be general enough to support a wide range of payloads. The emphasis was on having a single design to reduce satellite costs, but yet flexible enough that it would help reduce the time between payload design and the recovery of space data. Part of the flexibility would be attained by utilizing a programmable computer on the satellite. In this way, the satellite could provide services for different payloads whose needs might not be known until a few months before the mission. Where the needs are known (eg. see section 1) a programmable satellite could meet the different needs with little or no modification of the hardware. As an example, the computer could be programmed to provide different sequences of attitude control, sequences of equipment control, assign and reassign telemetry support, and provide experiment control. Computer controlled and operated satellites are relatively new and require more study and development, but could provide the answers to the problems presented by the wide range of experimental instruments and instrument requirements that are envisioned by the AMPS experimenters.

6.0 ACKNOWLEDGMENTS

It is a pleasure to acknowledge productive discussions with A. Hook, C. Rice and F. Morse of the Aerospace Corporation.

7.0 REFERENCES

1. D.F. Adamski, General-Utility Spacecraft and Multiple-Orbit/
Payload Launch Applications in Space Research and
Development, Aerospace Rept., TR-0158(3760-03)-1,
The Aerospace Corporation, Los Angeles, Calif., 1967.
2. Conceptual Design Study for Space Test Program Standard Satellite,
unpublished preliminary study, The Aerospace Corporation, 1975.
3. G.L. Duchossois, and D. Dale, AMPS-Subsatellite Study, Final
Report, European Space Research Organization, 1975.
4. W.B. Hanson, et al., The Atmosphere Explorer Satellite, Special
Issue of Radio Science, 8, p. 261, 1973.
5. F.A. Morse, et.al., Equatorial Ionospheric Irregularity Study
Satellite: EQUION Satellite, A Technical Proposal to NASA,
The Aerospace Corporation, Los Angeles, Calif., 1974.
6. Minutes of the AMPS Working Groups, September 1974-May 1975.

CONTENTS

	Page
1.0 INTRODUCTION	1
2.0 RECOMMENDATIONS	3
3.0 RADIATION RESISTANCES	5
3.1 Stationary Antenna	5
3.2 Moving Antenna	5
4.0 MAGNETIC LOOP ANTENNA	15
4.1 Weight and Impedance	15
4.2 Tuning Network	18
4.3 Radiation Efficiency	20
4.4 Power Amplifiers	25
4.5 Load Matching	29
5.0 ELECTRIC DIPOLE ANTENNA	31
5.1 Impedance	31
5.2 Radiation Efficiency	42
5.3 Power Amplifier and Load Matching	45
6.0 TRANSMITTER CONTROL CIRCUITRY	47
7.0 RAY PATHS EXCITED BY AN AMPS VLF TRANSMITTER	49
8.0 ACKNOWLEDGMENTS	55
9.0 REFERENCES	56

APPENDIX: Description of TVLF System Transmitter Control

1.0 INTRODUCTION

The Science Objectives of the Atmospheric, Magnetospheric, and Plasmas in Space (AMPS) payload for the Spacelab/Shuttle (Ref. 1) include a variety of objectives which will require a source of extremely-low-frequency (ELF) and very-low-frequency (VLF) waves. These waves will be used to study wave-particle interactions, to remotely probe the thermal plasma distribution, and to test existing theories of radiation in the space plasma environment.

The first phase of this portion of the study consisted of an overview of the literature related to ionospheric VLF wave sources. The most relevant information was found in material prepared as part of the U. S. Navy Sub-LF SATCOM Technology Development Program which analyzed a communications downlink in the 1 to 8 kHz frequency range (Ref. 2, 3, 4). Such a link contains a large number of distinct elements which must be modeled to arrive at the signal-to-noise ratio at a receiver. Some of these elements, such as coupling to the earth-ionosphere waveguide, D-region absorption, and sea-water penetration are not relevant to the experiments for which the AMPS facility is being designed. Unfortunately the data in Ref. 2 is presented as signal-to-noise ratios for a given power input without breaking out the different elements separately.

The following areas were identified as those which must be modeled in order to size a VLF antenna facility for AMPS: (1) The radiation resistance of candidate antennas, (2) the radiation pattern, (3) the impedance, and (4) the excitation of anomalous modes.

The radiation resistance calculations were discussed with Tom Wang of Stanford University. He recommended that we write computer programs based on his theoretical analyses to compute the radiation resistance for a loop and a dipole in a cold magnetoplasma (Ref. 5, 6). We have completed these programs using the mathematical formulations used by R. L. Smith at Develco (Ref. 2).

Radiation resistances were calculated for a magnetic loop antenna and for 40-m and 300-m tip-to-tip electric dipole antennas for eight plasma parameter sets which are representative of the environment at the AMPS orbit.

A total systems concept based on a realistic loop antenna configuration and on the 40-m and 300-m dipoles were formulated.

2.0 RECOMMENDATIONS

The following recommendations are a product of the VLF antenna study:

1. A magnetic loop antenna appears to be the most efficient wave source at VLF. We recommend that a loop antenna be incorporated in the AMPS payload and that a structural design compatible with the Spacelab be undertaken.
2. Although the power required from the power amplifier has been achieved from a solid-state device, an amplifier covering the range of output impedances required has not been fabricated. We recommend that a power-amplifier and load matching network, following the design outlined in Sections 4.3 and 4.4, be fabricated from flight qualified components and tested over the range of load impedances expected for the loop and dipole antennas.
3. That theories be developed and results obtained for the radiation pattern and loop antenna impedance for moving antennas oriented at arbitrary angles with respect to the geomagnetic field.
4. That theories be developed and results obtained for the radiation patterns and power radiated at frequencies above the lower-hybrid-resonance frequency.
5. That the field intensities from the loop antenna be computed at various angles and distances from AMPS to be used to select the sensitivity ranges of the receivers on the sub-satellites.

6. That a ray-tracing study be undertaken to determine the path followed by the whistler-mode waves. It is highly desirable to include a model for wave growth and damping along the ray path so that an estimate can be made of the wave-intensity at the geomagnetic equator. This information is required to properly design scientific experiments and to provide a time-line for operating the transmitters.
7. That the 300-m length is required to perform radiation studies on an electric-dipole antenna. The power radiated by the 40-m dipole is insignificant at frequencies below the low-hybrid-resonance. The 40-m dipole can be used for near-field and impedance studies.

3.0 RADIATION RESISTANCES

3.1 Stationary Antenna. The radiation resistances for a 40-m tip-to-tip electric dipole, a 300-m tip-to-tip electric dipole and a 12.6-m radius magnetic loop were calculated using the mathematical formulations developed by R. L. Smith at Develco (Ref. 2). Calculations were performed for eight ion-density models chosen to represent typical environments at altitudes of 300 and 500 km under day and night, and equatorial and mid-latitude conditions. The model parameters are shown in Table 1. The radiation resistances in ohms for the eight cases are shown in Tables 2 through 8. An assumption that the electric-dipole antenna is much shorter than a wavelength is violated when the wavelength condition in column two of each table exceeds 0.1. The columns headed "parallel" and "perpendicular" refer to the orientation of the dipole-moment vector with respect to the geomagnetic-field vector.

3.2 Moving Antenna. The ionospheric models developed in the study were provided to Dennis Baker at NRL to be used as inputs in an NRL computer code which calculates the radiation pattern of a VLF dipole antenna when the antenna is moving with respect to the ionosphere. The program can only be applied to the case of a dipole oriented parallel to the geomagnetic field moving parallel to the magnetic field.

Preliminary results for this restricted condition show maximum Doppler shifts of 8 Hz at 4 kHz when the LHR frequency is 4.67 kHz. The program also calculates the power radiated into small solid angles. The power radiated into a given solid angle subtended by 0.25 deg. from the moving antenna is within one percent of the power radiated into the same solid angle from the stationary antenna. These preliminary results

Table 1. Ion density models for radiation resistance calculations.

		300 km				500 km			
		Equator		Midlatitude		Equator		Midlatitude	
		O ⁺	H ⁺	O ⁺	H ⁺	O ⁺	H ⁺	O ⁺	H ⁺
Density cm ⁻³	Day	1.2×10^6	---	2.4×10^6	---	10^5	2×10^3	6×10^4	10^3
	Night	1.2×10^6	---	4×10^5	---	3×10^4	5×10^3	7×10^4	9×10^3
Electron Gyrofrequency, kHz		800		1200		700		1100	
LHR Frequency, kHz	Day	4.65		6.98		4.51		6.42	
	Night	4.65		6.85		7.18		9.68	

IONOSPHERIC CONDITIONS

ALTITUDE= 300.0 KM

ELECTRON DENSITY= 1.20E+06 EL/CM

LOCAL TIME= 1200.00

CYROFREQUENCY= 800.0 KHZ

MAG. LAT.= 0.0 DEG

LHR FREQUENCY= 4.652 KHZ

F (KHZ)	LENGTH(M)= 40.0			LENGTH(M)= 300.0			RADIUS(M)= 12.6		FREE SPACE		
	LENGTH COND	DIPOLE ANTENNA		LENGTH COND	DIPOLE ANTENNA		LOOP ANTENNA		40.0M DIPOLE	300.0M DIPOLE	12.6M LOOP
		PARALLEL	PERP		PARALLEL	PERP	PARALLEL	PERP			
1.0	2.1E-02	1.3E-37	1.7E-01	1.2E+00	7.5E-06	9.7E+00	5.3E-04	1.4E-04	3.5E-05	2.0E-04	9.6E-13
2.0	4.2E-02	5.4E-05	1.7E+00	2.4E+00	3.1E-04	9.8E+01	4.7E-03	1.2E-03	1.4E-05	7.9E-04	1.5E-11
3.0	6.3E-02	6.7E-35	9.6E+00	3.6E+00	3.3E-13	5.4E+02	1.9E-02	5.0E-03	3.2E-05	1.8E-03	7.8E-11
4.0	8.5E-02	9.3E-04	7.5E+01	4.8E+00	5.3E-12	4.2E+03	6.9E-02	1.8E-02	5.6E-05	3.2E-03	2.5E-10

Model I and II

Table 2. Radiation resistances in ohms for candidate antennas at 300 km altitude and equatorial latitudes during daytime and nighttime.

ORIGINAL PAGE IS
OF POOR QUALITY

IONOSPHERIC CONDITIONS

ALTITUDE= 300.0 KM

ELECTRON DENSITY= 2.40E+06 EL/CM

LOCAL TIME= 1200.00

CYROFREQUENCY= 1200.0 KHZ

MAG. LAT.= 45.0 DEG

HR FREQUENCY= 6.976 KHZ

F (KHZ)	LENGTH(M)= 40.0			LENGTH(M)= 300.0			RADIUS(M)= 12.6		FREE SPACE		
	LENGTH COND	DIPOLE ANTENNA		LENGTH COND	DIPOLE ANTENNA		LOOP ANTENNA		40.0M	300.0M	12.6M
		PARALLEL	PERP		PARALLEL	PERP	PARALLEL	PERP	DIPOLE	DIPOLE	LOOP
1.0	2.7E-02	3.5E-33	1.0E-01	1.5E+00	2.3E-06	5.9E+00	6.4E-04	1.7E-04	3.5E-06	2.0E-04	9.6E-13
2.0	5.5E-02	1.3E-35	9.2E-01	3.1E+00	7.1E-05	5.2E+01	5.5E-03	1.4E-03	1.4E-35	7.9E-04	1.5E-11
3.0	8.4E-02	1.1E-35	3.7E+00	4.7E+00	6.4E-04	2.1E+02	2.0E-02	5.2E-03	3.2E-05	1.8E-03	7.8E-11
4.0	1.1E-01	6.5E-05	1.2E+01	6.3E+00	3.5E-03	6.5E+02	5.3E-02	1.4E-02	5.6E-05	3.2E-03	2.5E-10
5.0	1.4E-01	3.2E-04	3.7E+01	7.9E+00	1.9E-02	2.1E+03	1.2E-01	3.2E-02	8.8E-05	4.9E-03	6.0E-10
6.0	1.7E-01	2.0E-35	1.6E+02	9.5E+00	1.1E-01	8.9E+03	2.9E-01	7.5E-02	1.3E-04	7.1E-03	1.2E-09

Model III

Table 3. Radiation resistances in ohms for candidate antennas at 300 km altitude and midlatitudes during daytime.

IONOSPHERIC CONDITIONS

ALTITUDE= 300.0 KM ELECTRON DENSITY= 4.00E+05 EL/30
 LOCAL TIME= 2400.00 GYROFREQUENCY= 1200.0 KHZ
 MAG. LAT.= 45.0 DEG LHR FREQUENCY= 6.850 KHZ

F (KHZ)	LENGTH(M)= 40.0			LENGTH(M)= 300.0			RADIUS(M)= 12.6		FREE SPACE		
	LENGTH COND	DIPOLE ANTENNA		LENGTH COND	DIPOLE ANTENNA		LOOP ANTENNA		40.0M DIPOLE	300.0M DIPOLE	12.6M LOOP
		PARALLEL	PERP		PARALLEL	PERP	PARALLEL	PERP			
1.0	4.5E-03	1.4E-33	4.3E-02	2.5E-01	8.1E-07	2.4E+00	4.3E-05	1.2E-05	3.5E-35	2.0E-04	9.6E-13
2.0	9.2E-03	5.1E-07	3.7E-01	5.2E-01	2.3E-05	2.1E+01	3.7E-04	9.8E-05	1.4E-35	7.9E-04	1.5E-11
3.0	1.4E-02	4.7E-35	1.5E+00	7.9E-01	2.5E-04	8.5E+01	1.4E-03	3.6E-04	3.2E-05	1.8E-03	7.8E-11
4.0	1.9E-02	2.6E-35	4.8E+00	1.1E+00	1.5E-03	2.7E+02	3.6E-03	9.3E-04	5.6E-05	3.2E-03	2.5E-10
5.0	2.3E-02	1.3E-34	1.5E+01	1.3E+00	7.3E-03	8.4E+02	8.4E-03	2.2E-03	8.8E-05	4.9E-03	6.0E-10
6.0	2.8E-02	8.1E-34	6.5E+01	1.6E+00	4.5E-02	3.6E+03	2.0E-02	5.1E-03	1.3E-04	7.1E-03	1.2E-09

Model IV

Table 4. Radiation resistances in ohms for candidate antennas at 300 km altitude and midlatitudes during nighttime.

ORIGINAL PAGE IS
OF POOR QUALITY

-6-

IONOSPHERIC CONDITIONS

ALTITUDE= 500.0 KM ELECTRON DENSITY= 1.02E+05 EL/CC
 LOCAL TIME= 1200.00 CYROFREQUENCY= 700.0 KHZ
 MAG. LAT.= 0.0 DEG HR FREQUENCY= 4.514 KHZ

F (KHZ)	LENGTH(M)= 40.0			LENGTH(M)= 300.0			RADIUS(M)= 12.6		FREE SPACE		
	COND	DIPOLE PARALLEL	ANTENNA PERP	COND	DIPOLE PARALLEL	ANTENNA PERP	LOOP PARALLEL	PERP	40.0M DIPOLE	300.0M DIPOLE	12.6M LOOP
1.0	2.0E-03	4.5E-03	4.5E-02	1.1E-01	2.5E-06	2.5E+00	1.5E-05	3.9E-06	3.5E-06	2.0E-04	9.6E-13
2.0	4.1E-03	1.8E-05	4.5E-01	2.3E-01	1.3E-04	2.5E+01	1.3E-04	3.5E-05	1.4E-05	7.9E-04	1.5E-11
3.0	6.1E-03	2.3E-03	2.5E+00	3.5E-01	1.3E-03	1.4E+02	5.5E-04	1.4E-04	3.2E-05	1.8E-03	7.8E-11
4.0	8.2E-03	3.3E-04	2.0E+01	4.6E-01	1.3E-02	1.1E+03	2.0E-03	5.1E-04	5.6E-05	3.2E-03	2.5E-10

-10-

Model V

Table 5. Radiation resistances in ohms for candidate antennas at 500 km altitude and equatorial latitudes during daytime.

IONOSPHERIC CONDITIONS

ALTITUDE= 500.0 KM ELECTRON DENSITY= 3.50E+05 EL/CC
 LOCAL TIME= 2400.00 SYNOFFREQUENCY= 700.0 KHZ
 MAG. LAT.= 0.0 DEG .HR FREQUENCY= 7.179 KHZ

F (KHZ)	LENGTH(M)= 40.0			LENGTH(M)= 300.0			RADIUS(M)= 12.6		FREE SPACE		
	COND	DIPOLE PARALLEL	DIPOLE PERP	COND	DIPOLE PARALLEL	DIPOLE PERP	LOOP PARALLEL	LOOP PERP	40.0M DIPOLE	300.0M DIPOLE	12.6M LOOP
1.0	6.6E-03	2.1E-03	2.1E-02	3.7E-01	1.2E-06	1.2E+00	5.6E-05	1.5E-05	3.5E-06	2.0E-04	9.6E-13
2.0	1.4E-02	7.3E-07	1.8E-01	7.7E-01	4.1E-05	1.0E+01	4.9E-04	1.3E-04	1.4E-05	7.9E-04	1.5E-11
3.0	2.1E-02	6.6E-05	7.3E-01	1.2E+00	3.7E-04	4.1E+01	1.8E-03	4.7E-04	3.2E-05	1.8E-03	7.8E-11
4.0	2.8E-02	3.6E-05	2.2E+00	1.6E+00	2.1E-03	1.3E+02	4.7E-03	1.2E-03	5.6E-05	3.2E-03	2.5E-10
5.0	3.5E-02	1.7E-04	6.7E+00	2.0E+00	9.5E-03	3.8E+02	1.1E-02	2.8E-03	8.8E-05	4.9E-03	6.0E-10
6.0	4.2E-02	9.1E-04	2.5E+01	2.4E+00	5.1E-02	1.4E+03	2.5E-02	6.3E-03	1.3E-04	7.1E-03	1.2E-09
7.0	4.9E-02	2.1E-02	4.1E+02	2.8E+00	1.2E+00	2.3E+04	8.8E-02	2.2E-02	1.7E-04	9.7E-03	2.3E-09

Model VI
 Table 6. Radiation resistances in ohms for candidate
 antennas at 500 km altitude and equatorial
 latitudes during nighttime.

ORIGINAL PAGE IS
 OF POOR QUALITY

IONOSPHERIC CONDITIONS

ALTITUDE= 500.0 KM
 LOCAL TIME= 1200.00
 MAG. LAT.= 45.0 DEG

ELECTRON DENSITY= 6.10E+04 EL/CC
 GYROFREQUENCY= 1100.0 KHZ
 LHR FREQUENCY= 6.419 KHZ

F (KHZ)	LENGTH(M)= 40.0			LENGTH(M)= 300.0			RADIUS(1)= 12.6		FREE SPACE		
	LENGTH COND	DIPOLE PARALLEL	ANTENNA PERP	LENGTH COND	DIPOLE PARALLEL	ANTENNA PERP	LOOP PARALLEL	ANTENNA PERP	+0.04 DIPOLE	300.0M DIPOLE	12.6M LOOP
1.0	7.5E-04	5.7E-03	1.4E-02	4.2E-02	3.2E-07	8.0E-01	2.7E-06	7.3E-07	3.5E-06	2.0E-04	9.6E-13
2.0	1.5E-03	2.0E-07	1.2E-01	8.6E-02	1.1E-05	7.0E+00	2.4E-05	6.2E-06	1.4E-05	7.9E-04	1.5E-11
3.0	2.3E-03	1.8E-15	4.9E-01	1.3E-01	1.1E-04	2.8E+01	8.6E-05	2.2E-05	3.2E-05	1.8E-03	7.8E-11
4.0	3.1E-03	1.0E-05	1.5E+00	1.7E-01	5.7E-04	8.6E+01	2.3E-04	5.8E-05	5.6E-05	3.2E-03	2.5E-10
5.0	3.9E-03	4.8E-15	4.7E+00	2.2E-01	2.7E-03	2.6E+02	5.2E-04	1.3E-04	8.8E-05	4.9E-03	6.0E-10
6.0	4.7E-03	2.7E-14	1.8E+01	2.6E-01	1.5E-02	1.0E+03	1.2E-03	3.0E-04	1.3E-04	7.1E-03	1.2E-09

Model VII

Table 7. Radiation resistances in ohms for candidate antennas at 500 km altitude and midlatitudes during daytime.

IONOSPHERIC CONDITIONS

ALTITUDE= 500.0 KM
 LOCAL TIME= 2400.00
 MAG. LAT.= 45.0 DEG

ELECTRON DENSITY= 7.90E+04 EL/CC
 GYROFREQUENCY= 1100.0 KHZ
 LHR FREQUENCY= 9.681 KHZ

-13-

F (KHZ)	LENGTH(M)= 40.0			LENGTH(M)= 300.0			RADIUS(M)= 12.6		FREE SPACE		
	LENGTH COND	DIPOLE PARALLEL	ANTENNA PERP	LENGTH COND	DIPOLE PARALLEL	ANTENNA PERP	LOOP PARALLEL	PERP	300.0M DIPOLE	300.0M DIPOLE	12.6M LOOP
1.0	9.2E-04	2.0E-09	5.2E-03	5.2E-02	1.1E-07	2.9E-01	2.6E-06	6.9E-07	3.5E-06	2.0E-04	9.6E-13
2.0	1.9E-03	6.7E-08	4.2E-02	1.1E-01	3.7E-06	2.3E+00	2.2E-05	5.8E-06	1.4E-05	7.9E-04	1.5E-11
3.0	3.0E-03	5.5E-07	1.5E-01	1.7E-01	3.1E-05	8.4E+00	7.8E-05	2.1E-05	3.2E-05	1.8E-03	7.8E-11
4.0	4.0E-03	2.6E-05	3.9E-01	2.2E-01	1.5E-04	2.2E+01	2.0E-04	5.1E-05	5.6E-05	3.2E-03	2.5E-10
5.0	5.0E-03	9.2E-05	8.9E-01	2.8E-01	5.1E-04	5.0E+01	4.1E-04	1.1E-04	8.8E-05	4.9E-03	6.0E-10
6.0	6.0E-03	2.8E-05	1.9E+00	3.4E-01	1.5E-03	1.1E+02	7.6E-04	2.0E-04	1.3E-04	7.1E-03	1.2E-09
7.0	7.0E-03	8.0E-05	4.0E+00	4.8E-01	4.5E-03	2.2E+02	1.3E-03	3.5E-04	1.7E-04	9.7E-03	2.3E-09
8.0	8.1E-03	2.4E-04	9.0E+00	4.5E-01	1.3E-02	5.0E+02	2.3E-03	6.0E-04	2.2E-04	1.3E-02	3.9E-09
9.0	9.1E-03	8.3E-04	2.5E+01	5.1E-01	4.7E-02	1.4E+03	4.2E-03	1.1E-03	2.8E-04	1.6E-02	6.3E-09

Model VIII

Table 8. Radiation resistances in ohms for candidate antennas at 500 km altitude and midlatitudes during nighttime.

indicate that the system design parameters we have been developing will be valid for geometries which can be realized near the geomagnetic equator. Although it is outside of the scope of this study, we are examining the theory for arbitrary antenna orientations and velocity directions with respect to the magnetic field. The number of wave modes which can be generated is extremely complex and we believe this information is required to satisfactorily perform scientific experiments and engineering measurements.

4.0 MAGNETIC LOOP ANTENNA

The radiation resistances tabulated in Table 9 suggest that an efficient antenna can be realized if the other losses in the antenna circuit are represented by resistances with values less than a few ohms. In order to achieve the radiation resistances shown in Table 9, the geometric area of the antenna must be equal to the area of the loop for which these calculations were performed. The loop area, πr^2 , is 499 m^2 . A triangular antenna of this area can be erected by the 50-m boom proposed for the AMPS Spacelab. The concept is shown in Fig. 1. If the base of the triangle is 20 m the area, $bh/2$, is 500 m^2 . If the triangle is a right triangle the perimeter is 123.85 m and the total cable length for a ten turn antenna is 1238.5 m.

4.1 Weight and Impedance. Copper is the best material to achieve the small dc resistance required. If the cable is manufactured from extra-flexible, rope-lay (7 × 98 × 32) #4 AWG, copper cable, the resistance is $8.45 \times 10^{-4} \Omega/\text{m}$ and the weight is 0.193 kg/m. This cable is 0.64 cm in diameter. The total resistance is 1.05Ω and the net weight is 239 kg. The ac and dc resistances at frequencies of a few kilohertz should be about equal. A possible alternative is the use of comparable copper tubing.

The net weight must be increased to account for the insulation, support material, and electrostatic shield which must surround the conductor bundle to minimize the excitation of electrostatic waves in the plasma.

The inductance of the antenna can be estimated using formulas for a similar configuration from Ref. 7. The closest figure is an isosceles triangle of equal area. The appropriate formula for the

Table 9. The radiation resistance in ohms of a ten turn loop antenna of radius 12.6 m at 4.0 kHz

	300 km		500 km	
	Equator	Midlatitude	Equator	Midlatitude
Day	6.9*	5.3	0.20*	0.72
Night	6.9*	0.36	0.47	0.62

* Lower hybrid resonance frequency is 4.6 kHz. The radiation resistance may include significant power lost in the resonance cones.

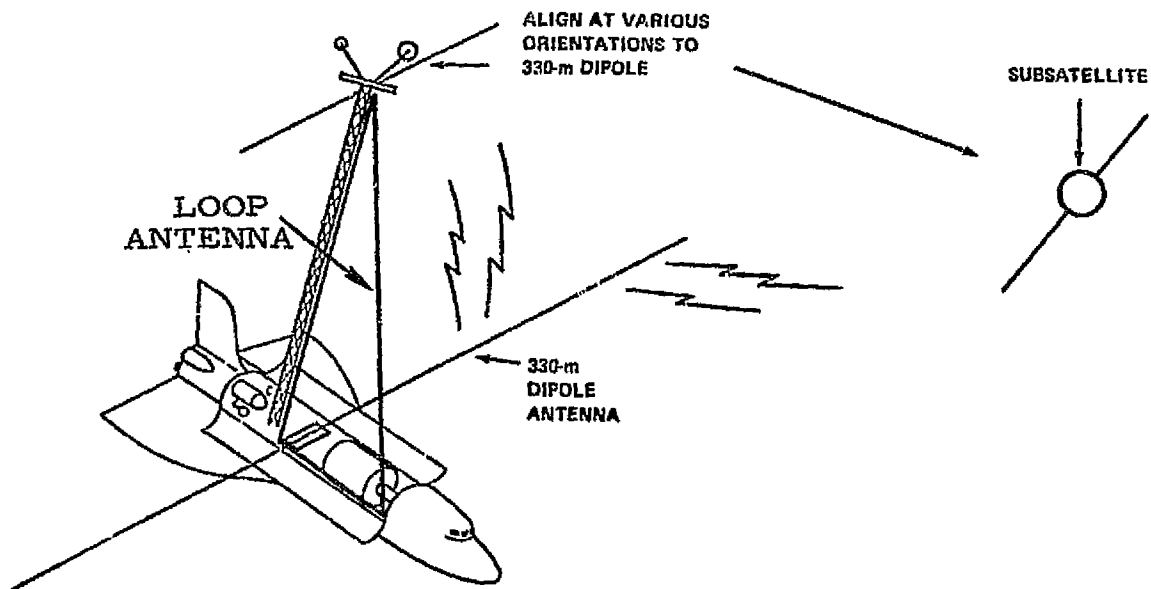


Fig. 1. Proposed loop antenna configuration for AMPS.

inductance is

$$L = 0.002 \ell \left[\ln \frac{2\ell}{\rho} - \alpha + 0.25 \right] \quad (1)$$

where ℓ is the perimeter in centimeters, ρ is the radius in centimeters, α is a constant which is characteristic of the figure and of its shape factor, and L is expressed in microhenries. For an isosceles triangle whose base is 20 m and whose height is 50 m, $\alpha = 3.62$. The inductance of a single turn as described in the preceding section is 195.6 μ H. If we assume that the ten turns are closely coupled the inductance is proportional to the square of the number of turns. The total inductance is then 19.6 mH.

4.2 Tuning Network. The inductive reactance of the antenna, ωL , is plotted in Fig. 2. At frequencies above 1 kHz the reactance is greater than 100 ohms. Hence it is necessary to tune the antenna with a series capacitor. The value of the capacitor is a function of frequency. It is given by

$$C = 1/\omega^2 L = 1.3 f^{-2} \quad (2)$$

where f is in Hertz. To cover the range from 300 Hz to 10 kHz requires a capacitor network from 1.3×10^{-8} F to 1.45×10^{-5} F.

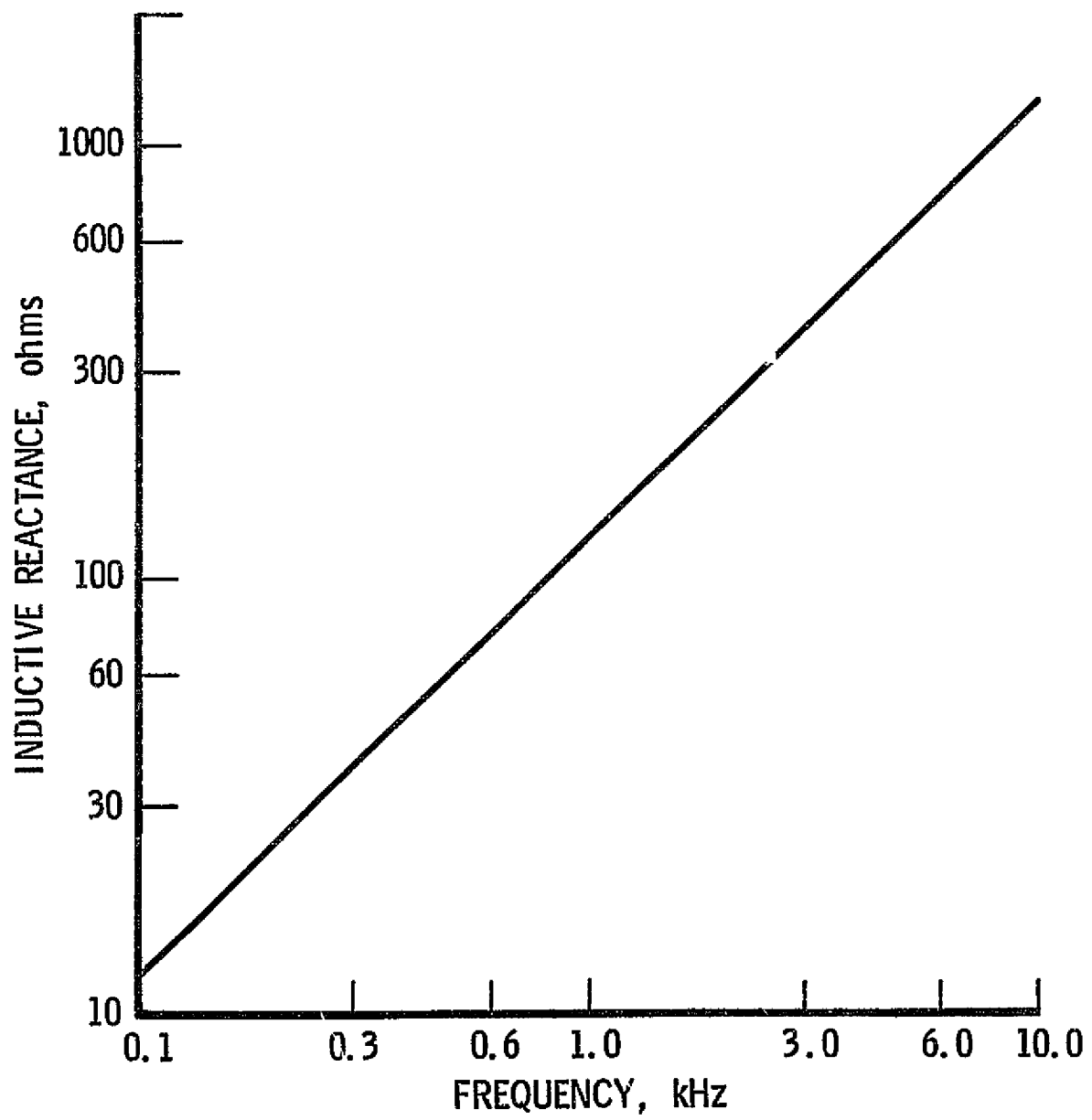


Fig. 2. Inductive reactance of 10-turn loop antenna proposed for AMPS.

4.3 Radiation Efficiency. Using the above results, the radiation efficiency can now be estimated. The efficiency is defined as

$$\eta = \frac{R_R}{R_R + R_{ac} + R_T} \quad (3)$$

where R_R is the radiation resistance, R_{ac} is the ac resistance of the copper cable, and R_T includes the effective resistance of the tuning circuit and other minor losses such as eddy currents in the vehicle skin. For R_R we will take (from Table 9) 0.36Ω at 4 kHz which is representative of midlatitude nighttime conditions at an altitude of 300 km. We take $R_{ac} = R_{dc} = 1.0 \Omega$. Although R_T cannot be obtained without actual measurements we can estimate the total losses based on our experience with similar antennas. We find that a Q of 50 is generally achievable. The effective resistance of the tuned circuit is then

$$R_{eff} = R_R + R_{ac} + R_T = \frac{\omega L}{Q} \quad (4)$$

The efficiency is then

$$\eta = \frac{R_R Q}{\omega L} \quad (5)$$

For our example at 4 kHz $\omega L = 485 \Omega$ and $\eta = 0.037$.

When the radiation resistance is much less than the other losses in the antenna system, the effective resistance of the tuned circuit, which is the load resistance as seen by the power amplifier, may be approximated by $\omega L/Q$ where Q may be practically taken to be 50. When the radiation is a significant fraction of the total losses in the circuit, the Q will be lowered and the effective resistance is better approximated as

$$R_{\text{eff}} = R_r + \frac{\omega L}{Q} = \frac{\omega L}{Q_{\text{eff}}} \quad (6)$$

where the Q excepting the losses due to radiation is still taken to be 50.

R_{eff} is plotted in Figure 2 for several of the ionospheric models. The values were calculated assuming $Q = 50$. For each case the lower bound to R_{eff} is $\omega L/Q$ and the upper bound becomes very large as the transmitter frequency approaches the lower-hybrid-resonance frequency.

The power radiated by the loop is

$$P_r = \frac{R_r}{R_{\text{eff}}} P_{\text{in}} \quad (7)$$

The power radiated for $P_{\text{in}} = 2 \text{ kW}$ is tabulated for the typical ionospheric parameters in Tables 10 and 11.

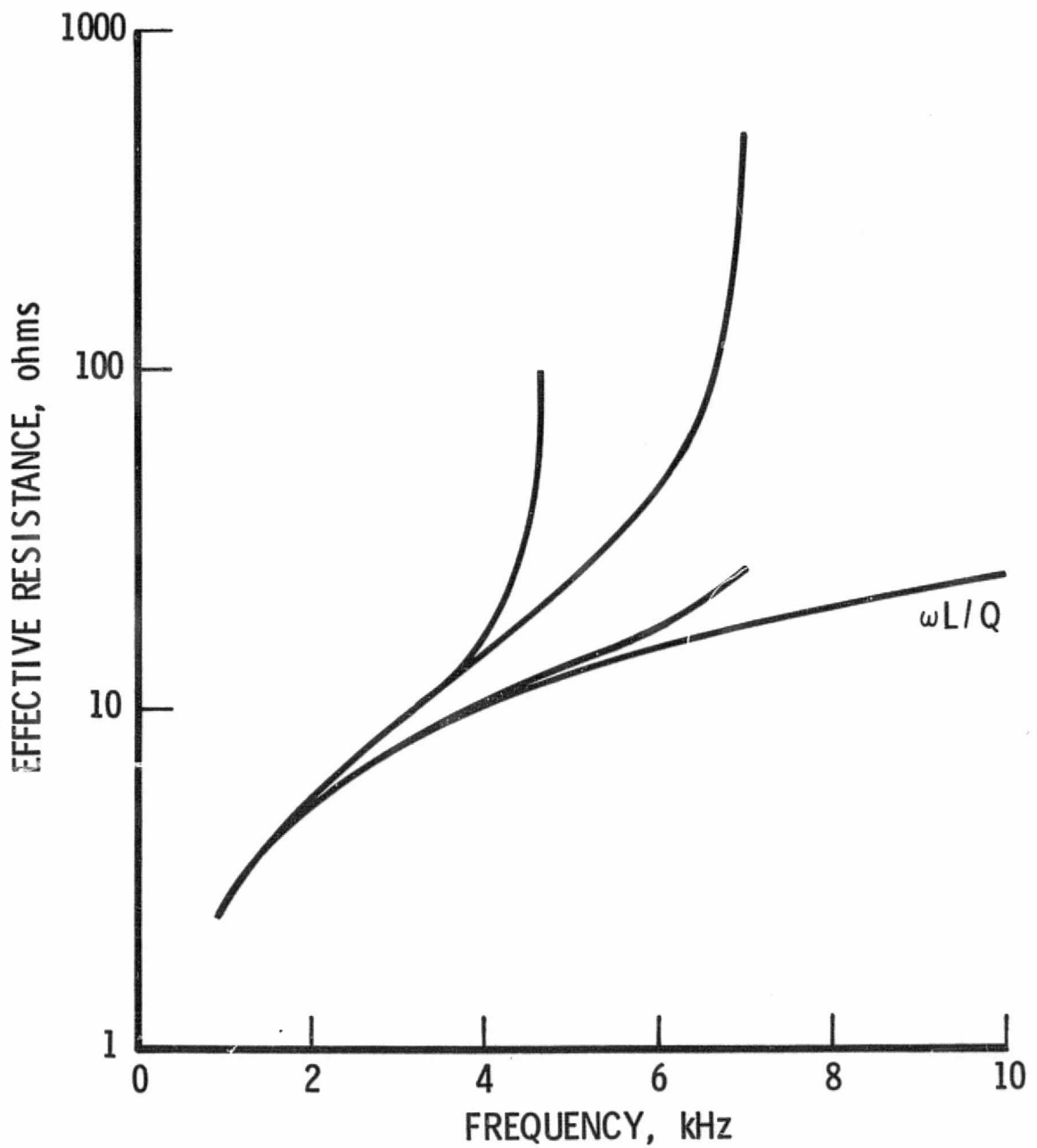


Fig. 3. The effective resistance for the tuned loop antenna circuit for several of the ionospheric models. The lower bound is $\omega L/Q$. Using cold plasma theory, the radiation resistance becomes infinite at the lower hybrid resonance frequency.

Table 10. Power Radiated by the Loop Antenna
at 300-km Altitude

FREQUENCY	ORIENTATION	
	PARALLEL	PERPENDICULAR
Model I, II	300 km - Equatorial -	Day and Night
1 kHz	42 W	11.4 W
2	190	44
3	408	126
4	820	308
Model III	300 km - Midlatitude -	Day
1 kHz	50 W	13.8 W
2	200	56
3	426	132
4	698	248
5	988	412
6	1324	672
Model IV	300 km - Midlatitude -	Night
1 kHz	3.4 W	1.0 W
2	14.8	4.0
3	38	9.6
4	70	18.6
5	128	36
6	238	66

Table 11. Power Radiated by the Loop Antenna
at 500-km Altitude

FREQUENCY	ORIENTATION	
	PARALLEL	PERPENDICULAR
Model V	500 km - Equatorial - Day	
1 kHz	1.2 W	.3 W
2	5.2	1.4
3	14.8	3.8
4	40	10.2
Model VI	500 km - Equatorial - Night	
1 kHz	4.6 W	1.2 W
2	19.8	5.2
3	48	12.6
4	90	24
5	164	44
6	290	82
7	676	232
Model VII	500 km - Midlatitude - Night	
1 kHz	.2 W	.06 W
2	.9	.24
3	2.2	.56
4	4.0	1.0
5	6.6	1.8
6	10	2.8
7	15	4.0
8	24	6.0
9	37	10

4.4 Power Amplifiers. The Tycobrahe Sound Co. of Hermosa Beach, California has fabricated a prototype audio amplifier which is suitable for driving the loop antenna. The load represented by the effective resistance of the circuit, $\omega L/Q$, is $9 \text{ } \Omega$ in the above example. This is typical of speakers used in audio sound systems and hence the technology is directly applicable. The prototype amplifier is solid state with an average power output of 2 kW. The unit is estimated to be 70% efficient. The power required to achieve maximum output is then 2.86 kW. The unit operates from a 110 V, 60 Hz line. This can be changed for Spacelab, however it may prove to be the most efficient and may not compromise the experiments since the EMI environment apparently precludes operating the receivers near the Spacelab. A higher input voltage may be required to achieve the full power output into a $10 \text{ } \Omega$ load. For 110 V input voltage, the present unit has an output voltage of $40 \text{ V}_{\text{rms}}$. Thus the output power is 160 W. This may be increased by redesigning the amplifier input or output circuits or by achieving a higher Q for the antenna circuit. The present unit measures 30.5 cm x 50.8 cm x 17.8 cm and weighs 20 kg. This light weight is achieved by using a transformerless design. The output stages consist of arrays of 3773 transistors mounted on Wakefield heatsinks. Although the heatsinks are presently air cooled, off-the-shelf liquid cooled heatsinks are available. The amplifier is claimed to be immune from damage due to open or short circuits.

This amplifier demonstrates that a 2-kW, solid-state, power amplifier is within the present state-of-the-art.

An evaluation of various techniques to amplify the signal, and match the signal to a tuned antenna is contained in Ref. 3. We find that, although that RCA study was specifically directed toward a small satellite and used an antenna impedance model which is now recognized as inappropriate for the dipole antenna, the basic recommendations are valid. The design parameters of the matching and tuning networks must be modified to conform to our present understanding of the impedance of the loop and dipole antennas. The Hybrid Power Module on which their recommended power amplifier was based was a developmental item in 1969. A similar module is now marketed by RCA Solid State Division. We will base our analysis on that device recognizing that similar devices are available from other manufacturers.

The Power Hybrid Circuit design is capable of delivering $2 \text{ kW}_{-2}^{+0} \text{ db}$ over the range of load resistances expected for the loop antenna at VLF was described by RCA (Ref. 3). Based on the data in Figure 3, a practical range of design load resistances is 2Ω to 200Ω . This can be achieved with an amplifier consisting of 24 Power Hybrid Circuits. This is the design recommended by RCA. It consists of twenty-four, 100-watt, class-B, push-pull amplifiers driven in parallel. Transformer-coupled outputs are combined in a load-matching circuit, using latching relays to provide a variety of series-parallel combinations. A specific combination is selected by logic according to the resistance measured at the tuner input.

The original RCA design was based on a developmental module RCA-TA7625. A similar device is now marketed by RCA Solid State Division. Quoting from the advertising brochure "The RCA-HC2000H 'Slash' Series types

are complete solid-state hybrid operational amplifiers in metal hermetic packages, especially designed for critical applications in aerospace, military, and industrial equipment." The device can provide up to 100 W output and up to 7A peak current. The bandwidth is 30 kHz at 60 W. It operates from a split power supply (± 37.5 V).

The recommended design selects a series-parallel combination of amplifier outputs to match the load resistance presented by the tuner. The mismatch loss is a function of the load resistance but is less than 2 dB over most of a 325:1 range of resistance. An attractive feature of the switched output configuration is the circuit redundancy which results in gradual failure characteristics.

The range of load resistances which can be driven by the amplifier matrix will range from a maximum value when all amplifiers are connected in series to a minimum value when all of the amplifiers are connected in parallel. The series HC200H/... devices are designed to drive a 4Ω load each.

Figure 4 (reproduced from Ref. 3) shows the capabilities of every useful series-parallel configuration with respect to power output and load resistance. In Figure 4 the power output is relative to the maximum available power from 24 amplifiers, and the load resistance is normalized with respect to the matched load for an individual amplifier. The specific configuration in Figure 4 is designated by the numbers 1 to 24 which is the number of series combinations of paralleled amplifiers. When the total number of series combinations does not divide evenly into 24, the effective number of amplifiers is less than 24.

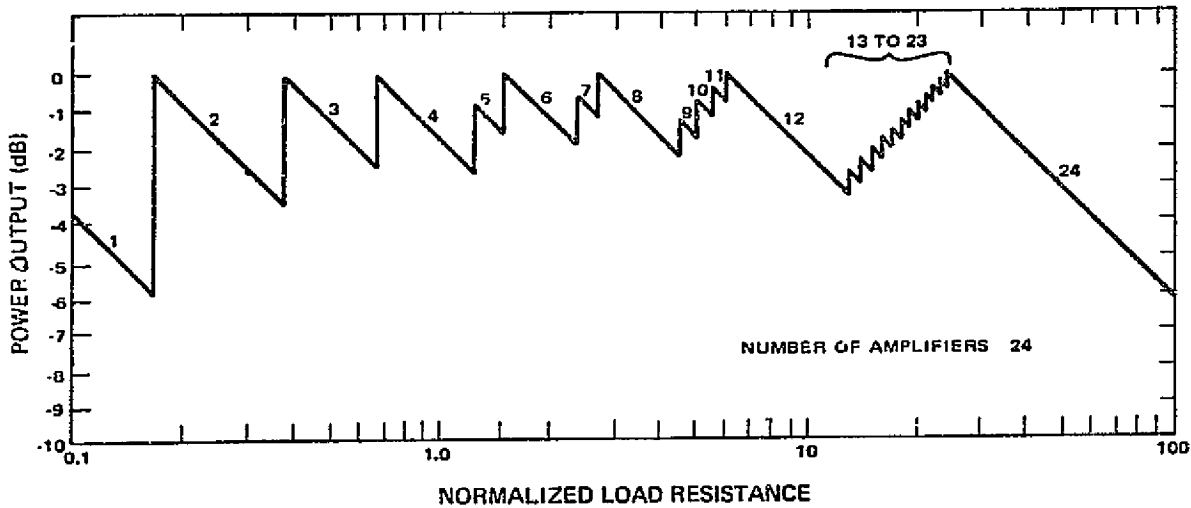


Fig. 4. Power output as a function of normalized load resistance. For the RCA-HC2000 H module the load resistance is 4Ω and the total power output for 24 modules is 2 kW. The range of actual load resistance covered by the graph is then 0.4 to 400Ω .

4.5 Load Matching. In the recommended switching scheme, the outputs of the amplifiers are combined by means of isolating transformers. This enables the amplifiers to operate from a single power supply and avoids the need for power supply switching. This approach does add weight and power loss in the isolating transformers.

The switching scheme is shown in Figure 5. The switches are double-pole double-throw latching relays. In position one the two adjacent inputs will be in parallel, in position two they will be in series.

RCA also considered two alternative matching schemes. They considered that the tapped transformer method has poor efficiency due to the transformer complexity. They also tested a variable transformer which they found had very poor efficiency above 10kHz at low brush positions.

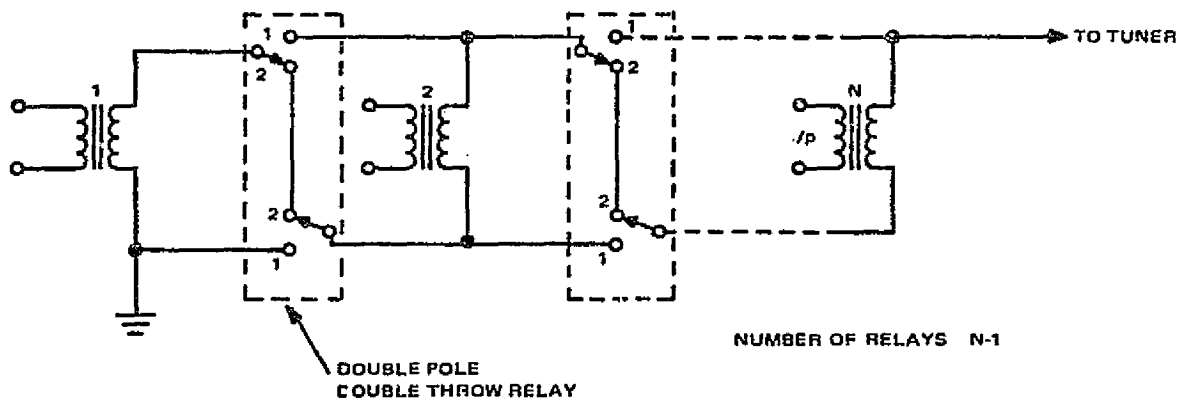


Fig. 5. Simplified Schematic of Power Amplifier Switching Method

5.0 ELECTRIC DIPOLE ANTENNA

5.1 Impedance. The impedance of an electric dipole antenna is complicated by the non-linear properties of the plasma sheath which surrounds the antenna in the ionosphere. Previous analyses have used a quasi-linear theory to calculate the impedance of the electric dipole (e. g. Ref. 8, 9). A satellite experiment aboard satellite OV1-21 showed that the magnitude of the impedance agreed reasonably well with the quasi-linear theory (Ref. 10). However the phase was a complicated function of frequency and driving voltage. At this time there is no adequate theory to evaluate the dynamic characteristics of the sheath.

We have developed an alternative approach to tuning an electric dipole antenna.

Shkarofsky (Ref. 8) estimates the sheath capacitance to be 10 pF/m and Develco (Ref. 2) uses the value 15 pF/m. For a 300-m tip-to-tip antenna the total capacitance would be 3000 pF to 4500 pF. The inductance $L = 1/\omega^2 C$ required to tune such an antenna to $\omega/2\pi = 2$ kHz is 1.4 H to 2.1 H.

We suggest that the sheath problem can be circumvented by loading the antenna circuit with a large capacitance, C_1 , as shown in Figure 6. In this configuration the sheath capacitance is only a small perturbation on the total circuit capacitance. The tuning is accomplished by resonating L with C_1 . The resulting high voltage across the sheath and radiation resistances should provide an adequate radiated power without the complex (perhaps impossible) servo system required to tune the sheath capacitance alone.

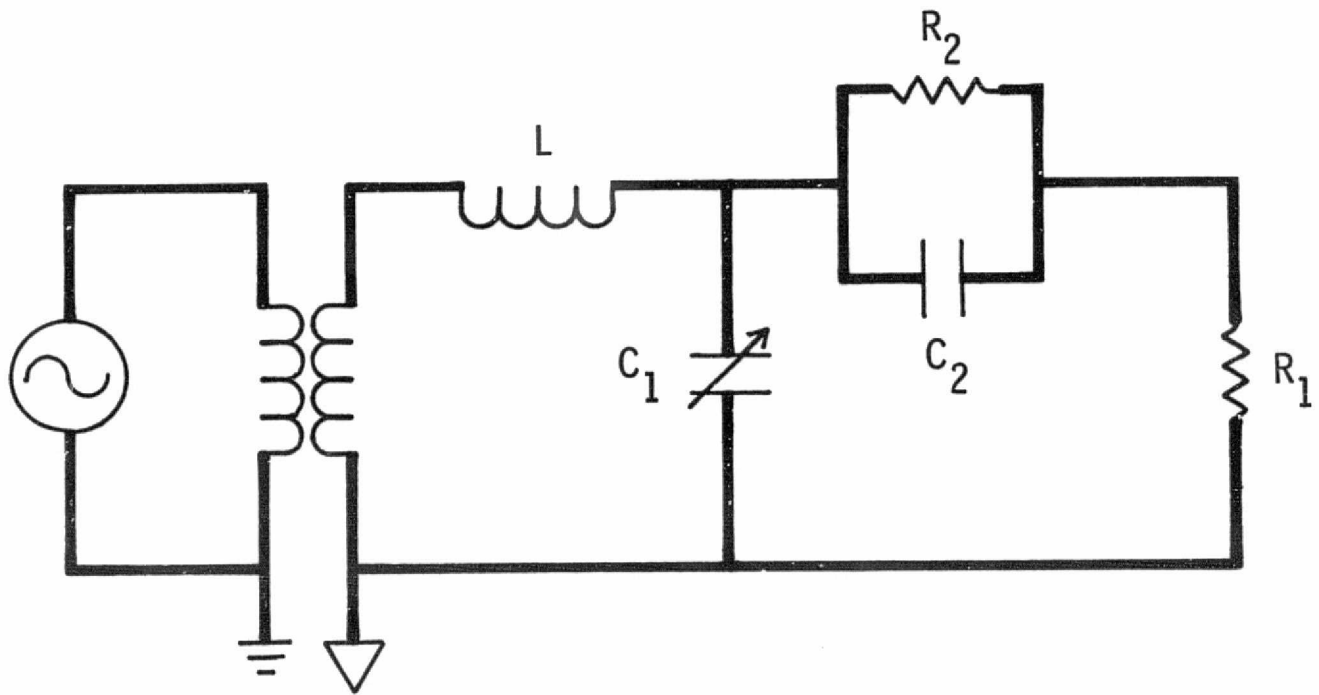


Fig. 6 Equivalent circuit for the electric dipole antenna in a magnetoplasma.

The input impedance of the circuit shown in Figure 6 is

$$Z_{in} = \frac{R_1 + R_2 + \omega^2 (R_2 C_2)^2 R_1}{(1 - \omega^2 R_1 C_1 R_2 C_2)^2 + \omega^2 [R_2 C_2 + C_1 (R_1 + R_2)]} + j\omega \left[L + \frac{(R_1 + R_2) R_2 C_2 + C_1 (R_1 + R_2) + R_1 R_2 C_2 (1 - \omega^2 R_1 C_1 R_2 C_2)}{(1 - \omega^2 R_1 C_1 R_2 C_2)^2 + \omega^2 [R_2 C_2 + C_1 (R_1 + R_2)]^2} \right]$$

(8)

This expression is unwieldy. Fortunately the results of the OV1-21 satellite experiment suggest further simplifications. As the driving voltage increased the measured impedance became insensitive to increases in the ambient plasma density (Ref. 10). This is evident in the data shown in Figure 7. At a frequency of 3.9 kHz and a driving voltage of 10V the impedance decreased a factor of three as the ion density increased from $2.5 \times 10^3 \text{ cm}^{-3}$ to $1.2 \times 10^5 \text{ cm}^{-3}$. At a driving voltage of 100 V the impedance only decreased 20 percent over the same density range. The increasing sheath conductance is primarily responsible for the decrease in the impedance as the ambient plasma density decreases. At the higher drive voltages the sheath conductance is greatly decreased because the region around the antenna is depleted of charge carriers. At the very high voltages (> 10 kV) expected to drive the AMPS electric-dipole antenna we expect the sheath conductance to be negligible.

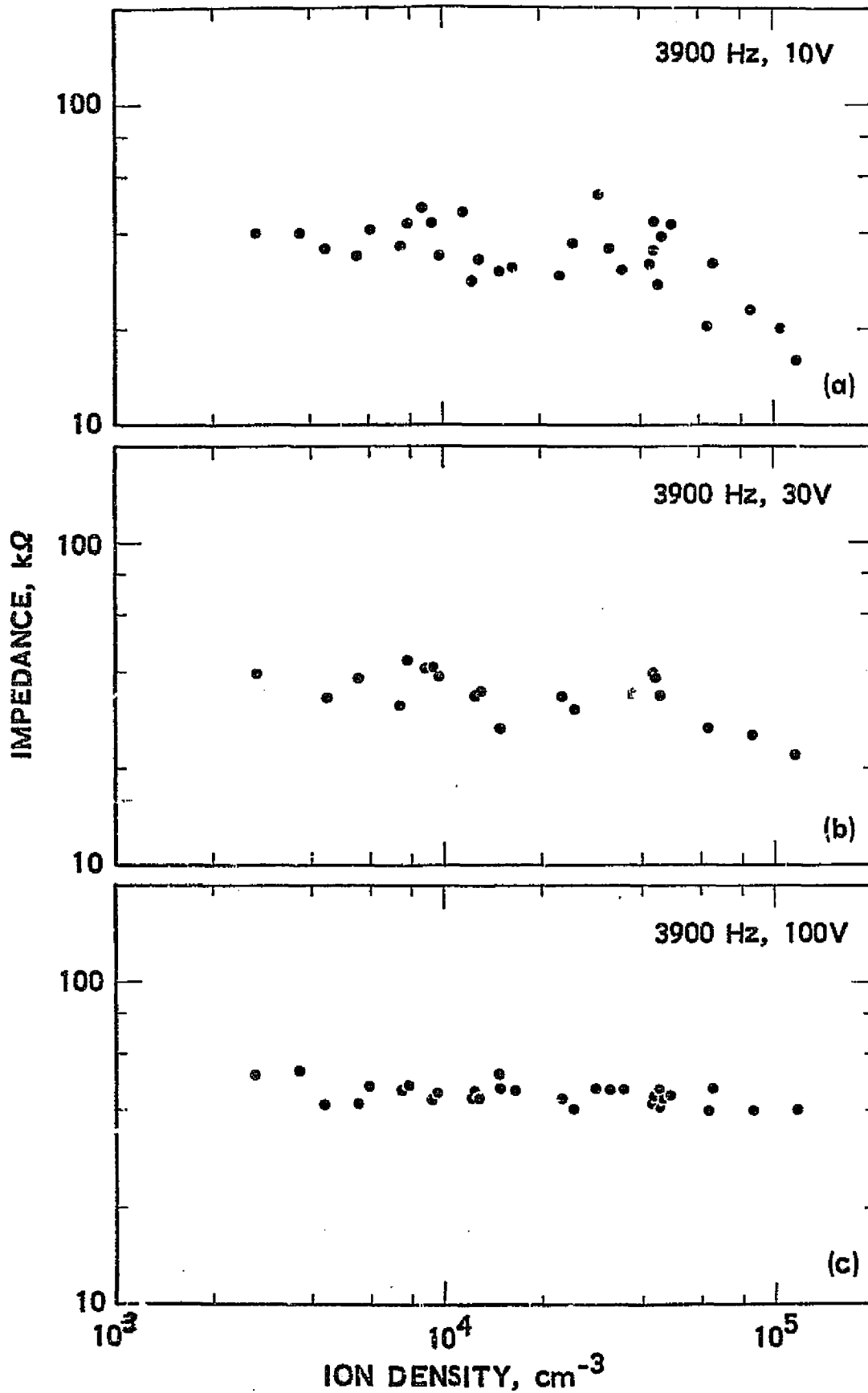


Figure 7. Magnitude of the dipole impedance for 10-, 30-, and 100-V excitation at 3.9 kHz as a function of total ion density.

We thus simplify the circuit in Figure 6 by allowing R_2 to go to infinity.

With this simplification the input impedance becomes

$$Z_{in} = \frac{R_1 C_1^2}{\omega^2 R_1^2 C_1^2 C_2^2 + (C_1 + C_2)^2} + j\omega \left[L - \frac{\omega^2 R_1^2 C_2^2 C_1 + C_1 + C_2}{\omega^4 R_1^2 C_1^2 C_2^2 + \omega^2 (C_1 + C_2)^2} \right] \quad (9)$$

The resonance frequency, ω_r , is given by

$$\omega_r^2 \approx \omega_0^2 \left[1 - \frac{\delta}{1 + \omega_0^2 \tau^2} \right] \quad (10)$$

where $\omega_0^2 = 1/L C_1$, $\delta = C_2/C_1$, and $\tau = R_1 C_2$. The assumption has been made that $\delta \ll 1$. The radiated power is

$$P_r = \frac{R_r |V_{in}|^2 \delta^2}{R_1^2} \left[1 + \omega_0^2 \tau^2 + \delta \left(\frac{2 + \omega_0^2 \tau^2}{1 + \omega_0^2 \tau^2} \right) \right] \quad (11)$$

where R_r is the radiation resistance which is contained within R_1 in the circuit shown in Figure 1. At resonance the impedance is

$$Z_r = \frac{R_1}{1 + 2\delta + \omega^2 \tau^2} \quad (12)$$

Our task now is to estimate the values of the circuit components for a realistic antenna. For a 300-m tip-to-tip dipole, we choose $C_2 = 3000$ pF using Shkarofsky's calculation as the best estimate (the OV1-21 satellite measurements agreed with Shkarofsky's theory at lower drive voltages -- in free space the value would be about 1500 pF.) Choose $C_1 = 10 C_2$ then $\delta = 0.1$.

We have discussed the resistance of a BeCu Stem Antenna with Ron Samuels of SPAR Aerospace. The dc resistance of a 300 meter stem, .635 cm in diameter and 3.8×10^{-3} cm thick is approximately 18Ω . The effective ac resistance, R_{AC} , for a sinusoidal current applied to the base of an electrically short antenna is one-third of the dc resistance. Hence $R_{AC} \approx 6 \Omega$.

For the radiation resistance we choose $R_r = 22 \Omega$ at 2 kHz corresponding to a dipole oriented perpendicular to the magnetic field at an altitude of 500 km at mid-latitudes during local day time (Table 9). The radiation resistance at 2 kHz ranged from 7.4Ω to 98Ω for the 300-m dipole for the eight cases we have studied.

If $R_1 = R_{AC} + R_r = 28 \Omega$ (this neglects the resistance of the tuning inductor which will be included below, and the power lost to anomalous plasma modes), then $\tau = 8.4 \times 10^{-8}$ sec and at 2 kHz, $\omega_0 \tau = 1.06 \times 10^{-3}$. For any reasonable values of the parameters, $\omega^2 \tau^2$ will be negligible over the VLF range.

Equations 10, 11, and 12 then simplify to

$$\omega_r^2 \approx \omega_0^2 [1 - \delta] \quad (13)$$

$$P_r = \frac{R_r |V_{in}|^2 \delta^2}{R_1^2} [1 + 2\delta] \quad (14)$$

and

$$Z_r = \frac{R_1}{1 + 2\delta} \quad (15)$$

The value of the inductor required to tune the circuit to 2 kHz is obtained from Equation 13.

$$L = (1 - \delta) / [(2\pi f_r)^2 C_1] = 0.19 \text{ H.}$$

In practice a Q of 50 can be realized in a tuning circuit for a relatively inefficient antenna. The effective resistance of the circuit at resonance is related to L and Q by

$$R_{\text{eff}} = \frac{L}{Q} = 48\Omega \quad (16)$$

At resonance $R_1 = R_{\text{eff}}$ and $Z_r = R_1/1.2$.

If 2 kw of power are delivered to the tuning circuit the base antenna current at resonance is

$$I = (P/R_{\text{eff}})^{1/2} = 6.5 \text{ A} \quad (17)$$

The input voltage is

$$V_{\text{in}} = IR = 312 \text{ V} \quad (18)$$

The voltage across the inductor is $\omega LI = 15.5$ kV. The power radiated is

$$P_r = \frac{22 \times 312^2 \times .1^2}{48^2} \left[1 + 2 (.1) \right] = 11 \text{ watts} \quad (19)$$

Although this appears to represent a very small output, successful ground based experiments have been conducted at this power level (Ref. 11). At 6.6 kHz the Transportable Very Low Frequency Transmitter Facility can radiate 100 W.

The modification to the input resistance at resonance for large radiation resistances introduced for the loop antenna has been incorporated here into the analysis of the electric-dipole antenna.

At resonance, the effective resistance of the tuned circuit is

$$R_{\text{eff}} = \frac{R_1}{1 + 2b} + \frac{\omega L}{Q} = \frac{L}{Q_{\text{eff}}} \quad (20)$$

where $R_1 = R_r + R_{ac}$. R_{eff} is plotted as a function of frequency for the 40-m and 300-m dipoles in Figs. 8 and 9 respectively. The inductance required to tune the circuit to resonance at a frequency f_r is

$$L = (1 - S) / \left[(2\pi f_r)^2 C_1 \right] \quad (21)$$

The inductance required for the 40-m and 300-m dipoles is plotted as a function of frequency in Fig. 10. If the power delivered to the tuning circuit is P_{in} , then the input current to the tuning network is

$$I_{\text{in}} = (P_{\text{in}}/R_{\text{eff}})^{1/2} \quad (22)$$

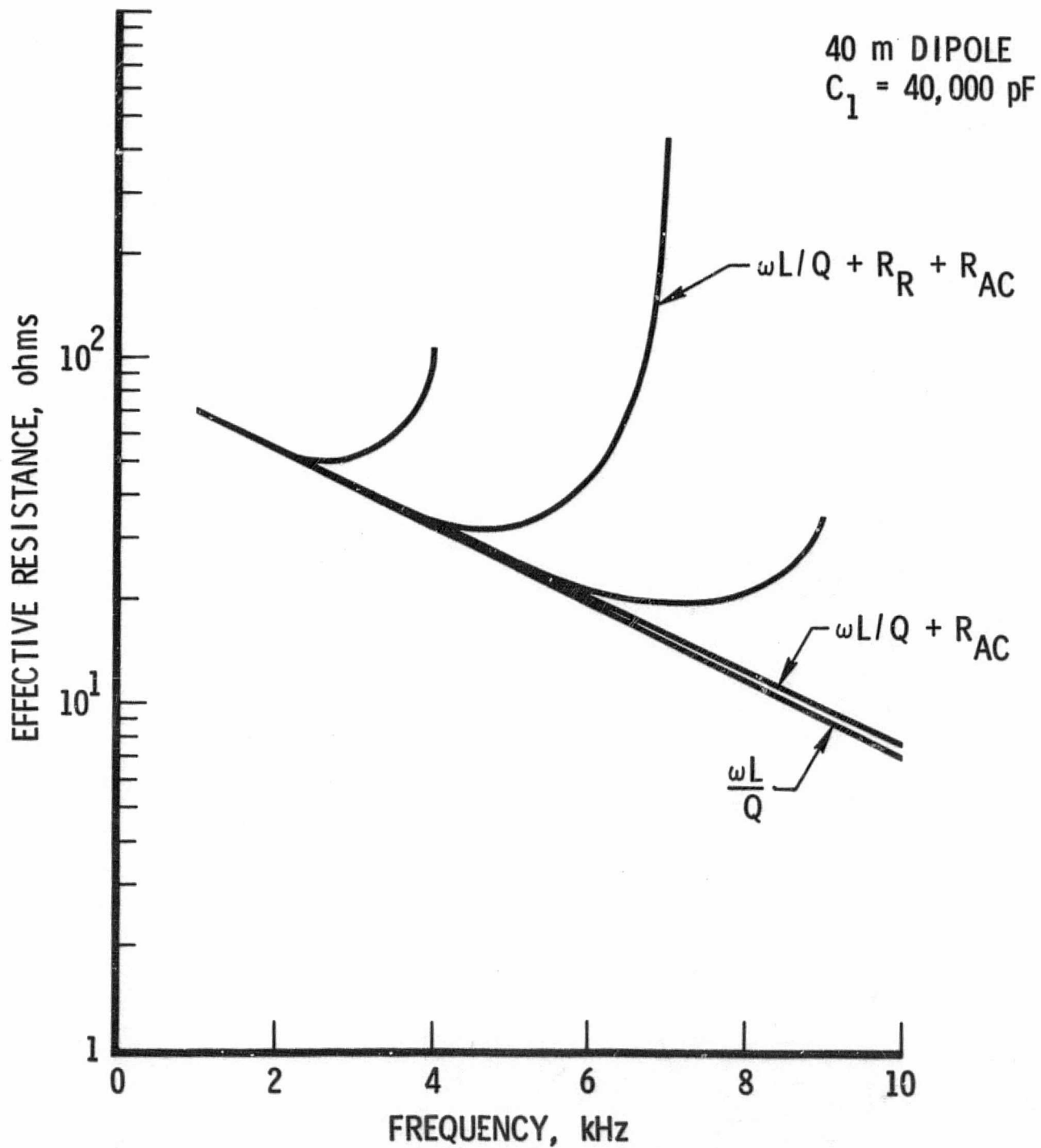


Fig. 8. The effective resistance of the 40-m electric dipole antenna as a function of frequency for several of the ionospheric models.

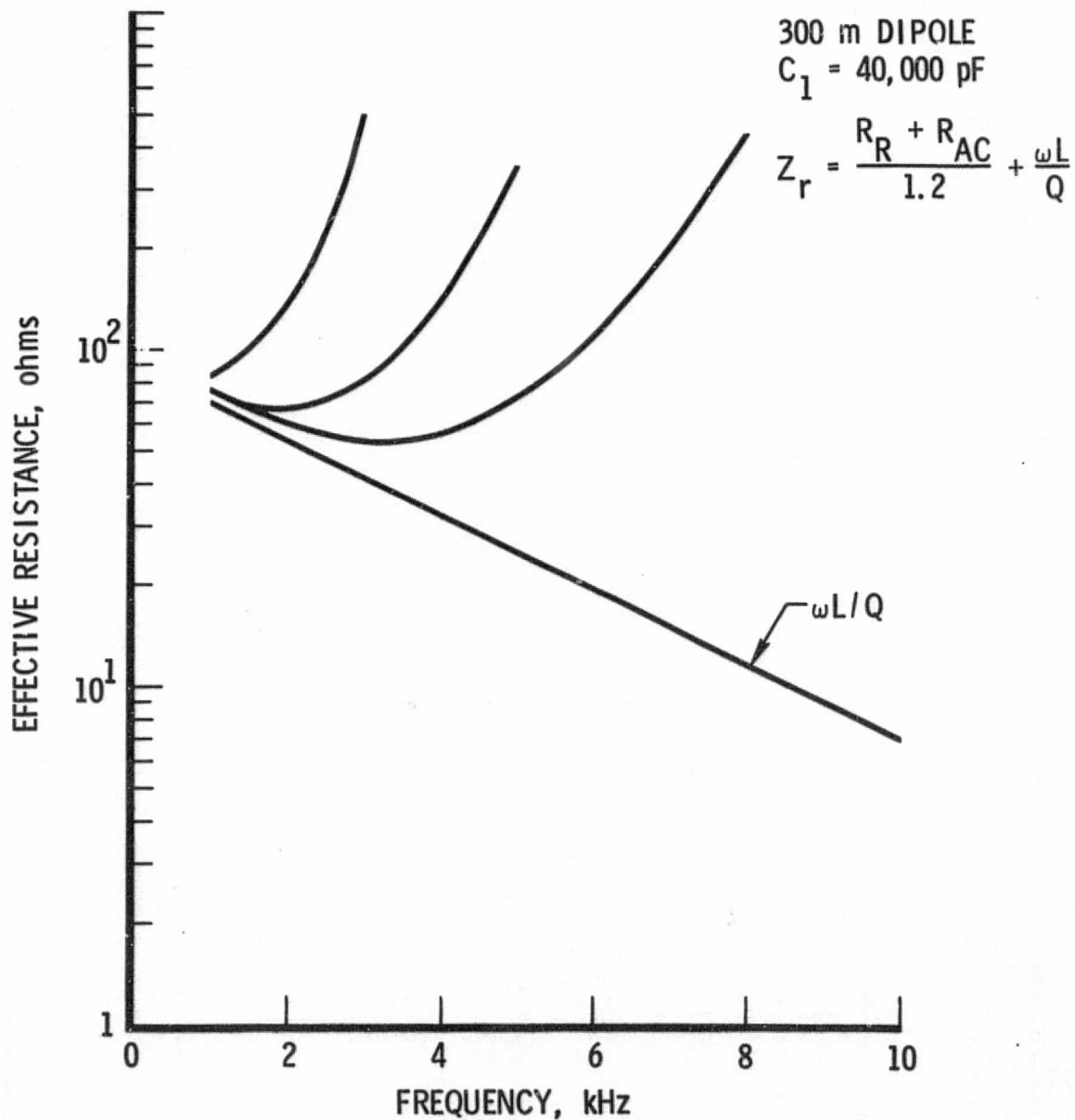


Fig. 9. The effective resistance of the 300-m electric dipole antenna as a function of frequency for several of the ionospheric models.

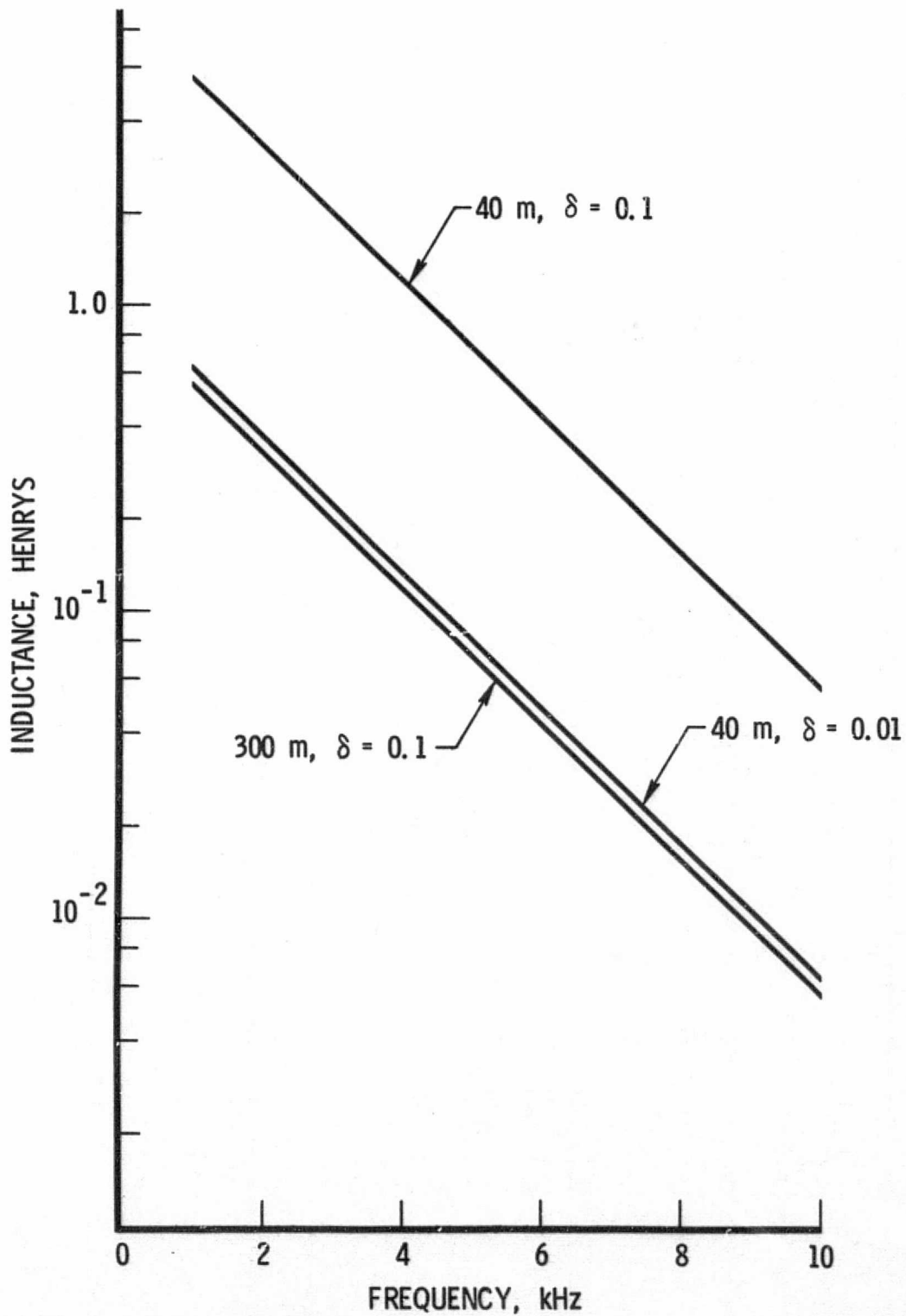


Fig. 10. Inductance required to tune the electric dipole antennae as a function of frequency.

C-2
The input voltage is

$$V_{in} = I_{in} R_{eff} \quad (23)$$

The power radiated is

$$P_r = \frac{R_r |V_{in}|^2 \delta^2}{R_{eff}^2} \left[1 + 2\delta \right] \quad (24a)$$

$$= I_{in}^2 R_r \delta^2 \left[1 + 2\delta \right] \quad (24b)$$

It is clear from Equ. 24 that capacitive loading (δ small) significantly reduces the current that flows through the antenna.

5.2 Radiation Efficiency. We have calculated the power radiated by a 40-m and a 300-m dipole under voltage-limited and power-limited conditions. These are two of the three practical limits in high-power VLF engineering. Under the range of conditions encountered in the ionosphere, the electric dipole will never be current limited. The base-voltage limit is established by the insulating hardware at the base of the antenna. For a typical ground-station installation, the practical limit is 75 to 100 kV. We consider a practical limit for AMPS to be 50 kV based on our experience with the TVLF facility. Although it is conceivable that a 100 kV limit could be attained, our calculations indicate that the total power dissipated in the circuit would exceed 2 kW before the base voltage exceeds 50 kV.

An upper limit to the radiated power can be calculated from the current through the radiation resistance under base-voltage limiting conditions. Under these conditions, the current is limited by the reactive impedance of the sheath which greatly exceeds the ohmic and radiation impedances in the antenna. The numerical results are presented in Table 12.

For all of the conditions considered in this study, the radiated power from the 300-m antenna is limited by the total power available from the power amplifier. At the lowest frequencies, the power radiated by the 40-m antenna is limited by the base voltage. However, at the higher frequencies it is limited by the total power available to the circuit.

Table 12. Circuit Parameters and Power Radiated Under Base-Voltage Limited Conditions. The Base-Voltage is Taken to be 50 kV.

Antenna Length	40 m	300 m
Sheath Capacitance	400 pF	3000 pF
Capacitive Reactance		
1 kHz	400 k Ω	53 k Ω
4 kHz	100 k Ω	13 k Ω
10 kHz	40 k Ω	5.3 k Ω
Base Current		
1 kHz	0.125 A	0.94 A
4 kHz	0.5 A	3.8 A
10 kHz	1.25 A	9.4 A
Radiation Resistance		
1 kHz	0.005 - 0.1 Ω	0.3 - 9.7 Ω
4 kHz	0.39 - 75 Ω	22 - 1100 Ω
Power Radiated		
1 kHz	to 7.8 x 10 ⁻⁵ W 1.6 x 10 ⁻³ W	0.27 - 8.6 W
4 kHz	to 9.8 x 10 ⁻² W 18.8 W	317 - 15,884 W

Table 13 contains the numerical results under the assumption that the total power available to the matching network is 2 kW.

5.3 Power Amplifier and Load Matching. In this section we described a power amplifier design, based on Power Hybrid Circuits, which is capable of delivering 2 kW_{-2}^{+0} db over the range of load resistances expected for the loop antenna at VLF. For the loop antenna, the load resistance varied from 2 to 200Ω except at the lower hybrid resonance where the load resistance became very large. For the 300-m dipole the load resistance varies from 10Ω (at 10 kHz with $R_r = 0$) to 110Ω (at 1 kHz with $R_r = 9.7 \Omega$). Thus, the power amplifier and load matching network design described for the loop antenna is also applicable to the 300-m dipole. The load resistance of the 40-m dipole exceeds 400Ω at frequencies below 4 kHz, hence a significant power mismatch will result. Since the power radiated by the 40-m dipole is extremely small at frequencies below 4 kHz, it should not be necessary to modify the design to accommodate the 40-m antenna circuit at those frequencies.

Table 13. Circuit Parameters and Radiated Power Under the Assumption That the Total Power Available to the Tuning Network is 2 kW.

Antenna Length	40 m	300 m
Radiation Resistance		
1 kHz	0.005 - 0.1 Ω	0.3 - 9.7 Ω
4 kHz	0.39 - 75 Ω	22 - 1100 Ω
Effective Resistance ($\delta = 0.1$)		
1 kHz	955 Ω	100 - 109 Ω
4 kHz	239 - 302 Ω	47 - 95 Ω
Total Current		
1 kHz	1.45 A	4.5 - 4.3 A
4 kHz	2.9 - 2.6 A	6.5 - 2.1 A
Base Voltage		
1 kHz	69.2 kV	21.2 - 20.5 kV
4 kHz	34.6 - 30.7 kV	7.8 - 2.5 kV
Power Radiated		
1 kHz	to 1.3 x 10 ⁻⁴ W 2.5 x 10 ⁻³ W	0.7 - 2.1 W
4 kHz	0.04 - 5.9 W	11.2 - 58.8 W

6.0 TRANSMITTER CONTROL CIRCUITRY

The transmitter is keyed by a programmer which is synchronized to Coordinated Universal Time. The power amplifier is driven by a frequency synthesizer which can be programmed in frequency and amplitude. The programmer must also control the antenna tuning circuit.

A block diagram of the transmitter control circuit is shown in Fig. 11. Similar functions are performed by instruments included in the transportable very-low-frequency (TVLF) transmitter facility operated by The Aerospace Corporation (Ref. 12). The frequency synthesizer in that facility is a Hewlett Packard Model 3320 B (Dimensions: 42.5 x 49.2 x 13.3 cm, weight 15.4 kg).

The programmer is driven by the Time Code Generator which is a Datatron Model 3000. The time code generator is driven by the oscillator in the frequency synthesizer which is more stable than the oscillator in the time code generator itself.

On Spacelab the program might be provided by the Spacelab computer. Alternatively a special purpose programmer similar to the one in the TVLF facility might be fabricated. A description of the programs incorporated in the TVLF unit are included in the Appendix. The TVLF unit was constructed by Prof. Dowden, University of Otago, Dunedin, New Zealand. A unit for the Spacelab would have the approximate dimensions 25 x 25 x 10 cm and weigh 4 kg.

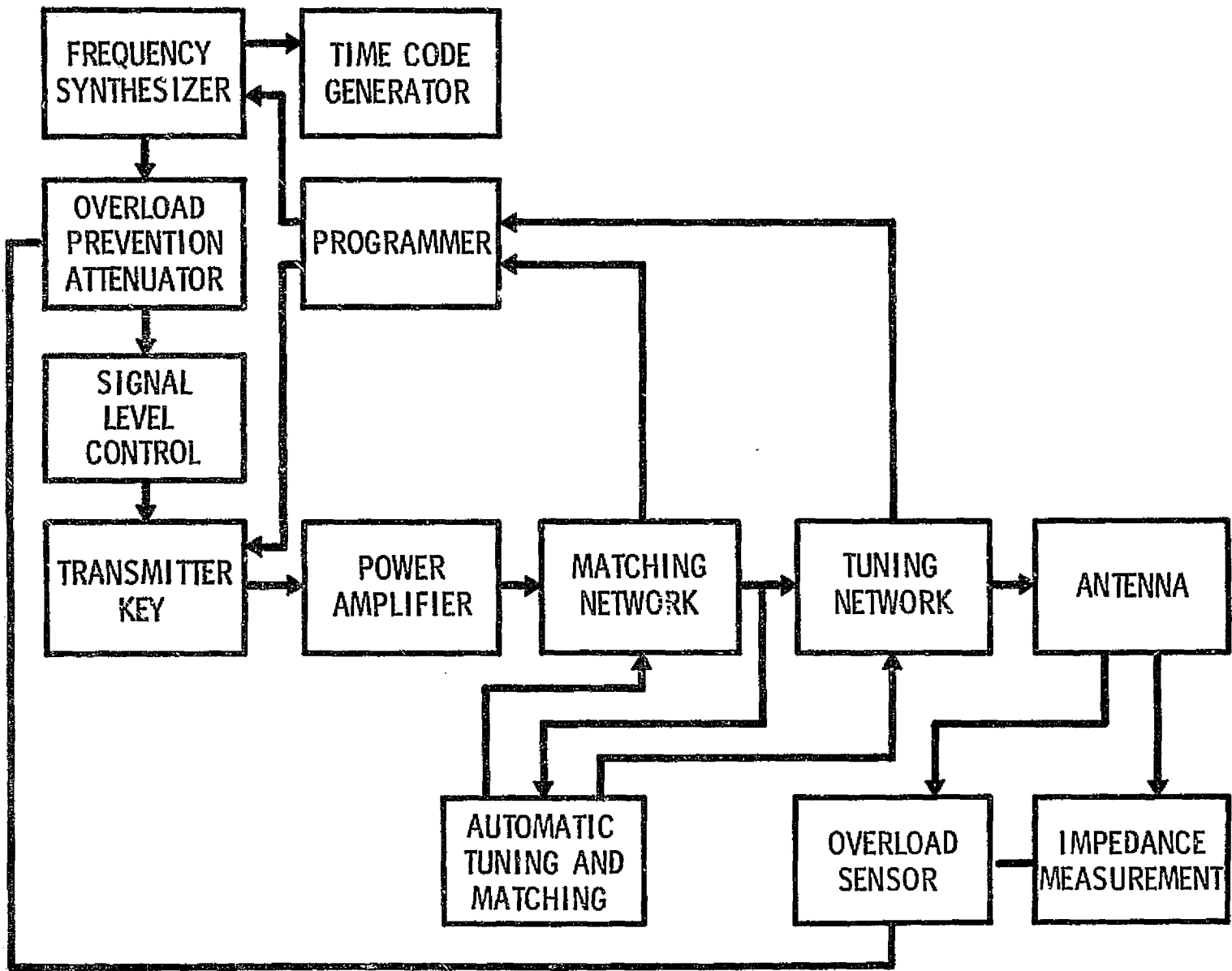


Fig. 11. Block Diagram of Transmitter Control Circuitry

7.0 RAY PATHS EXCITED BY AN AMPS VLF TRANSMITTER

Bruce Edgar of the Space Physics Laboratory has been undertaking a very preliminary analysis of the ray-paths traveled by whistler-mode waves transmitted by a satellite-borne VLF transmitter. He will be presenting a paper titled "Sounding the Magnetosphere with a Satellite Borne VLF Transmitter" at the 1975 USNC/URSI Meeting. Although this work was not supported by the current NASA contract, we include an example of the results here to indicate the complexity of the results. We believe that a significant effort in this area will be required in order to scientifically exploit the capabilities of the VLF transmitter.

We will consider the case of a shuttle location at 45° N magnetic latitude and at 500-km altitude. Figure 12 shows the refractive index surface conditions at 3 kHz for an ionosphere having a composition of 90% O^{+} - 10% H^{+} ion and a total electron density of $7.9 \times 10^4 \text{ cm}^{-3}$. The refractive index surface is a plot of μ , the refractive index as a function of wave-normal angle and is symmetric about the magnetic field vector \vec{B}_0 .

The refractive index surface also defines the initial direction of the ray paths. We assume that all wave normal angles will be excited by the antenna. (Whether this assumption is entirely correct, should be an area of future research.) For each wave normal angle (defined here as δ , the angle between \vec{F} and \vec{p}) one can define a ray direction which is perpendicular to the refractive index surface as shown in the example of Figure 12. Since the refractive index surface is highly elongated in a direction perpendicular to \vec{B}_0 , the majority of the ray directions are contained in a cone about \vec{B}_0 .

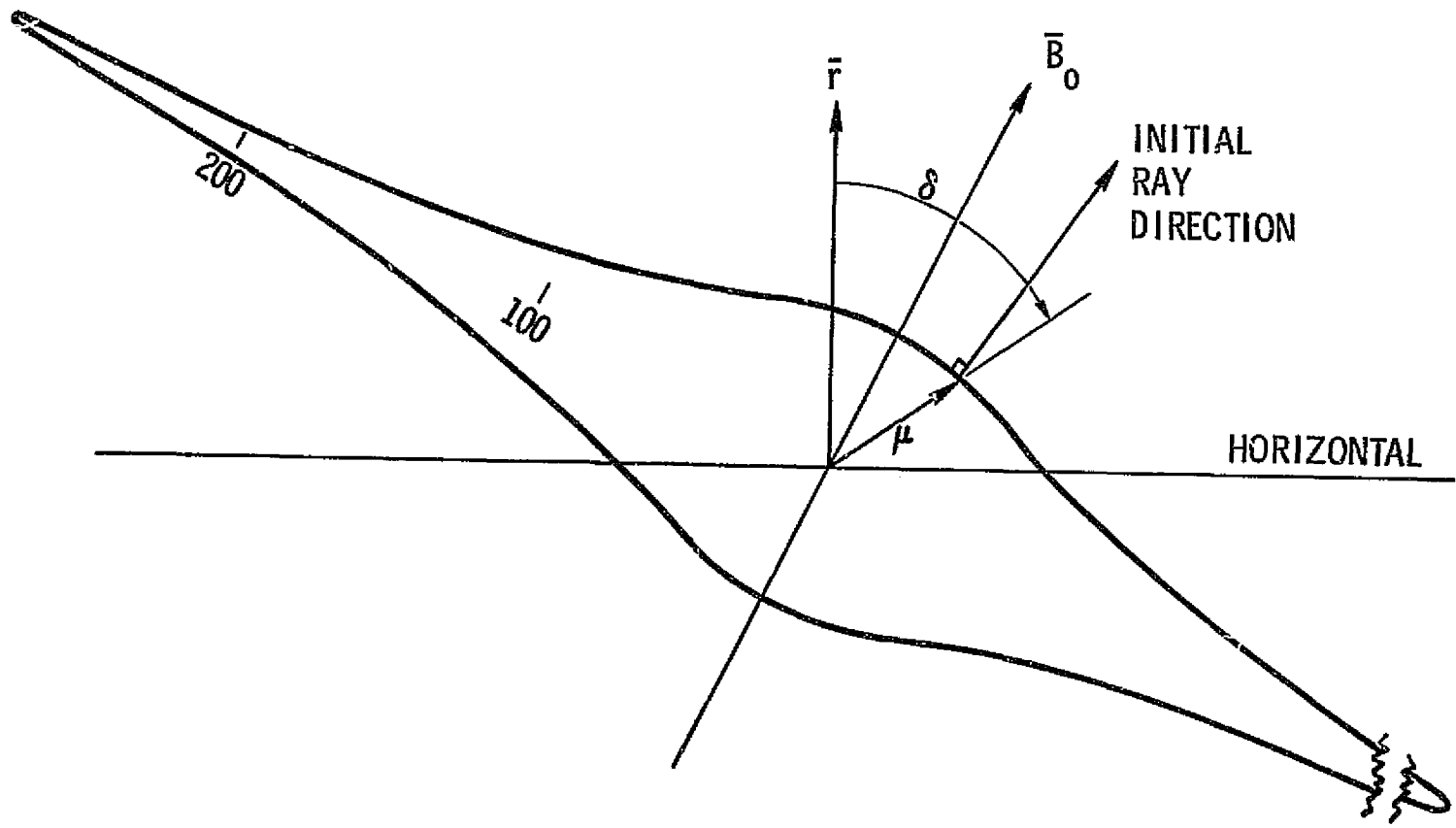


Fig. 12. Refractive index surface at shuttle location. The vector F is the radius vector directed outwards from the center of the earth. The wave normal angle δ is measured clockwise from F . The initial ray direction is perpendicular to the refractive index surface.

Figure 13 shows the ray paths from the shuttle to the upper magnetosphere. The angles denote the initial values of δ , the wave normal angle. The magnetospheric density followed a diffusive equilibrium model using the ion composition and a constant base density level mentioned in the introduction. The ray path calculations were arbitrarily ended at 3 seconds. Some of the ray paths ($20^\circ \leq \delta \leq 80^\circ$) undergo magnetospheric reflections in Figure 13. The other ray paths will also undergo magnetospheric reflections, but at times, greater than 3 sec.

Figure 14 shows the modification of the ray paths by a plasma-pause at $L \sim 4$. The plasma-pause essentially contains the ray paths and prevents the ray paths from initially crossing $L \sim 4$. The electron gradient structure of the magnetosphere has a large effect upon the type of ray paths that can be excited.

The ray paths that reach the lower ionosphere are plotted in Figure 12. The ray paths for $\delta = 100^\circ$ and 110° allow the shuttle to transmit to lower latitudes, but there is a region of exclusion for the higher latitudes as shown by Figure 15. This latter fact is inherent to the quasi-field aligned nature of VLF propagation and cannot be overcome by antenna design, etc.

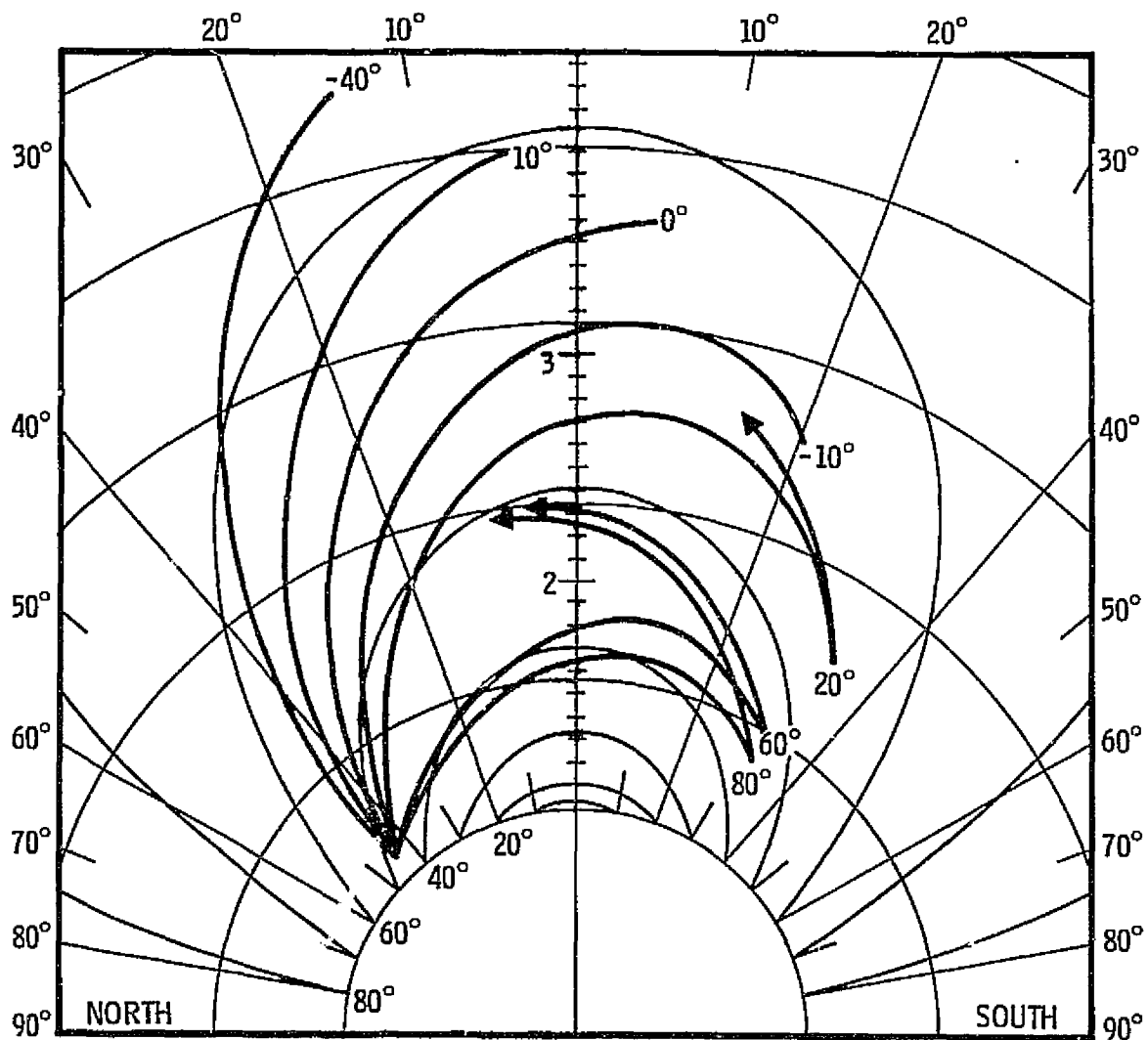


Fig. 13. Ray paths from the shuttle to the outer magnetosphere at 3 kHz. The angles beside each path denote the initial value of the wave normal angle δ for each case. The calculations assume a diffusive equilibrium density model with a constant base level density.

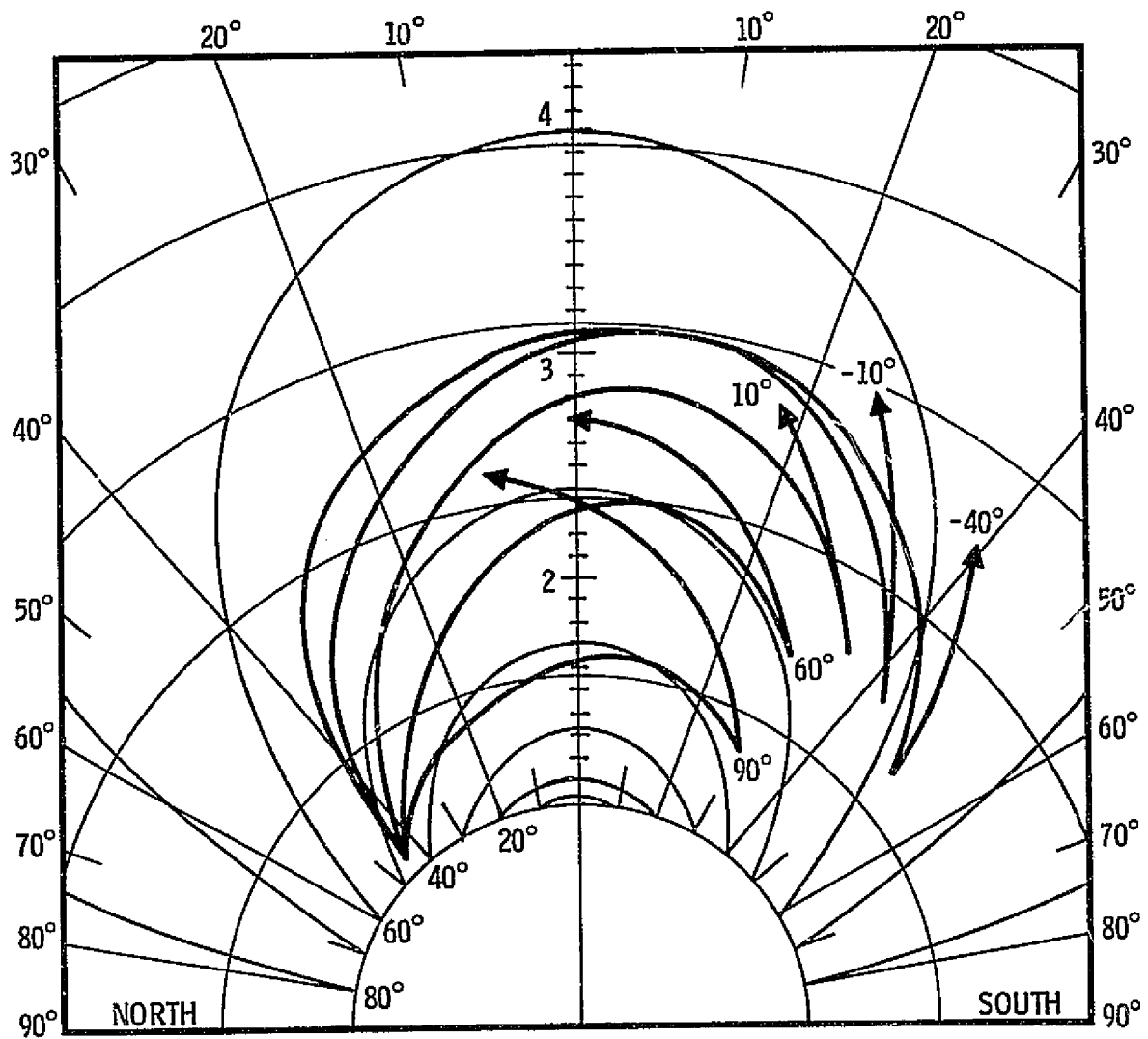


Fig. 14. Ray paths from the shuttle to the outer magnetosphere with a plasmopause location at $L \sim 4$. The ray paths are essentially contained inside $L \sim 4$ by the electron density gradients of the plasmopause.

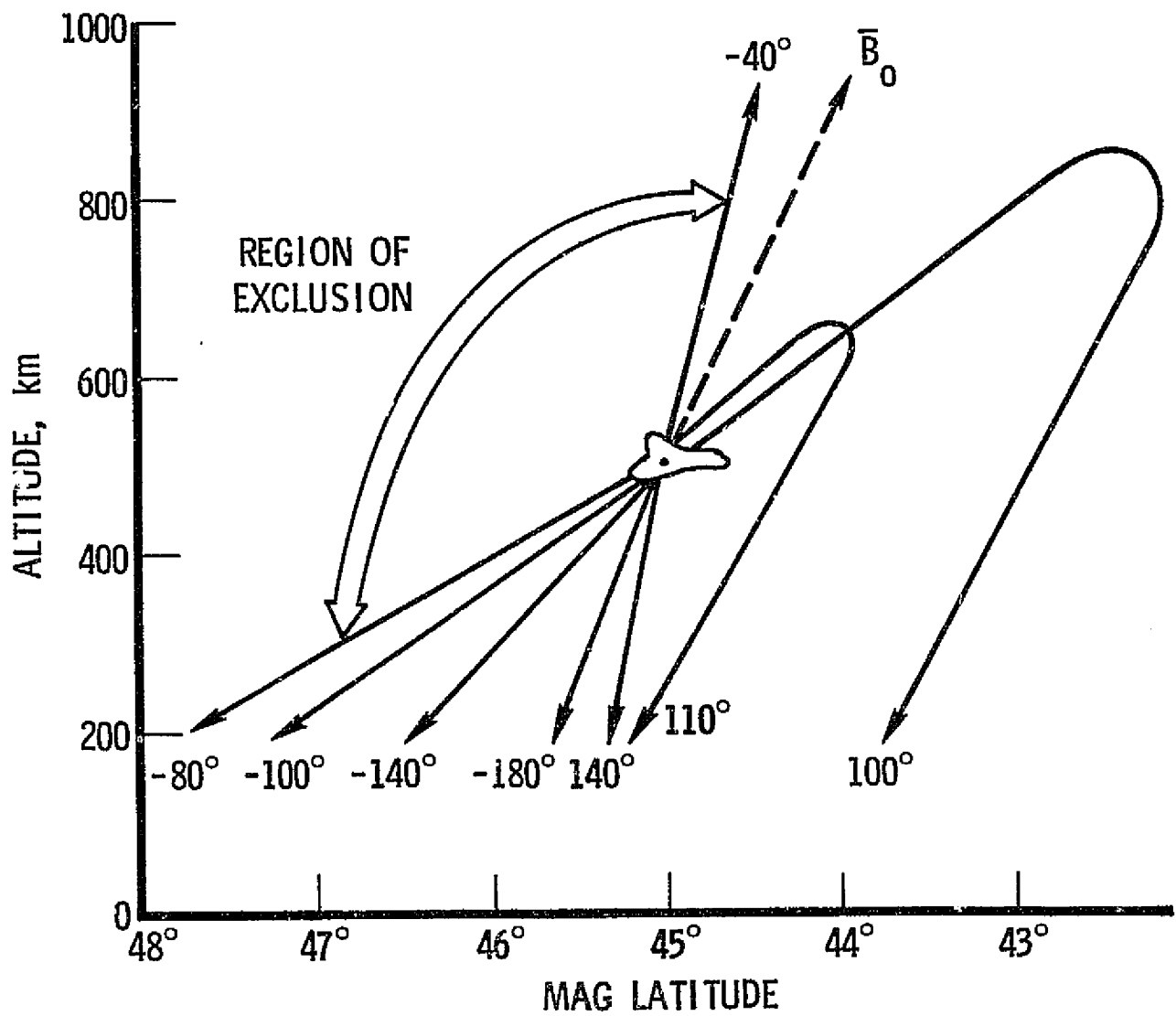


Fig. 15. Ray paths to the lower ionosphere. The region between the $\delta = -80$ and $\delta = -40$ ray paths defines a region of exclusion for VLF propagation.

8.0 ACKNOWLEDGMENTS

We are indebted to B. C. Edgar for the computer calculations of the radiation resistances and ray tracing, and to D. Baker (NRL) for computer calculations of radiation from a moving antenna. It is a pleasure to acknowledge productive discussions with T. N. C. Wang, (Stanford University), R. Samuels (SPAR Aerospace), M. H. Dazey, and W. B. Harbridge.

9.0 REFERENCES

1. C. R. Chappell, O. Garriott, and S. Bauer, Science Objectives of the Atmospheric, Magnetospheric and Plasmas in Space (AMPS) Payload for the Spacelab/Shuttle, (private communication in draft form), 1975.
2. L. H. Rorden, et al., The Feasibility of a Sub-LF Satellite-to-Submarine Communications Downlink (U), Develco Report No. 532-720731, Mountain View, California (31 July 1972) (Secret).
3. ELF/VLF Propagation Spacecraft Experiment Design Study Final Report, RCA Defense Electronic Products, Astro Electronics Division, Report No. 70-226-(56), October 27, 1969. (Secret)
4. L. S. Bearce, "Some Considerations Related to the Feasibility of ELF/VLF Downlink Satellite Communications, "Proc. Conf. Antennas and Transionospheric Propagation as Related to ELF/VLF Downlink Satellite Communications, Naval Research Laboratory Report 7462, Washington, D. C., 27 November 1972.
5. T. N. C. Wang and T. F. Bell, On VLF radiation resistance of an electric dipole in a cold magnetoplasma, Radio Sci., 5, 605-610, 1970.
6. T. F. Bell and T. N. C. Wang, Radiation resistance of a small filamentary loop antenna in a cold multicomponent magnetoplasma, IEEE Trans Antennas Propagat., AP-19, 517, 1971.

7. F. W. Grover, Inductance Calculations, D. Van Nostrand Company, Inc., New York, 1946.
8. I. P. Shkarofsky, Nonlinear Sheath Admittance, Currents and Charges Associated with High Peak Voltage Drive on a VLF/ELF Dipole Antenna Moving in the Ionosphere, Radio Sci., 7, 503 (1972).
9. D. Baker, H. Weil, and L. S. Bearce, Impedance and Large Signal Excitation of Satellite-Borne Antenna in the Ionosphere, IEEE Transactions on Antennas and Propagation AP-21, 672-679, 1973.
10. H. C. Koons and D. A. McPherson, Measurement of the nonlinear impedance of a satellite-borne, electric dipole antenna, Radio Science, 9, 547-558, 1974.
11. D. A. McPherson, H. C. Koons, M. H. Dazey, R. L. Dowden, L. E. S. Amon, and N. R. Thomson, Alaska to New Zealand whistler-mode transmission at 6.8 kHz, Nature, 248, 493, 1974.
12. H. C. Koons and M. H. Dazey, Transportable VLF Transmitter, in ELF-VLF Radio Wave Propagation, edited by J. Holtet, D. Reidel Publishing Co., Dordrecht, Holland, P. 413, 1974.

APPENDIX: DESCRIPTION OF TVLF
SYSTEM TRANSMITTER CONTROL

Transmitter On/Off Control

This Multi-Function Unit (MFU) is designed to provide all desired pulse programmes including morse code and manual control. The special feature of the pulses is that all are derived from the 1 MHz clock so that all leading and trailing edges occur at precisely known times (in U.T.) and in synchronism with the Dunedin unit.

Installation. Mount in rack for reasonable air circulation (cooling is by convection only). Plug in *POWER*, 1 MHz *IN* (from H.P. Synthesiser or elsewhere, $\Delta 1p.p.s.$ from Astrodata OR $-1p.p.s.$ from Datatron. The Binary Clock will then synchronise automatically all functions faster and including 1 p.p.s. so the light emitting diode (LED) marked *SEC* should flash on in synchronism with Astrodata (or Datatron) seconds.

Complete synchronisation of the Binary Clock (and so the rest of the Multi Function Unit) with the Alaskan clock or time code generator (Astrodata or Datatron) requires the manual procedure given below. *Minute synchronisation should be checked at least once each day as spontaneous errors sometimes occur.*

Minute Synchronisation. At any time within about 15 seconds before a U.T. (Universal Time or GMT) minute, press red button marked "SYNC ENABLE". LED will come ON, indicating an "armed" condition for the next 20 seconds or so. Then immediately after

the U.T. minute ("00" seconds) but before 01 seconds, press the green button marked SYNC. LED will go OFF. Check that the LED marked MIN flashes on for 1 second at later U.T. minutes ("00" sec.). Both of these buttons work only on pressing so the green SYNC button need not be released before 01 seconds.

All functions (sweeper, repetitive pulser) will now be synchronised with U.T. and so with the identical unit at Dunedin (we expect synchronisation at Dunedin to be within 1 m.sec. of U.T.).

Repetitive Pulse Mode (Binary clock panel)

Select the desired pulse repetition rate from any one of (rotary switch on front panel marked PULSE REPETITION):

32, 16, 8, 4, 2, 1 pulses per sec. 2, 5, 10, 30, 60 sec. per pulse CW (continuous on or "key down").

Select the desired pulse length from any one of (*PULSE LENGTH* rotary switch)

1/64, 1/32, 1/16, 1/8, 1/4, 1/2.

1, 2, 5, 10, 30 seconds duration, SQ (automatically 1:1 mark/space)*.

LED labelled MARK will flash ON to indicate the TTL "true" pulse available for keying the transmitter. The toggle switch marked *DEFINE MARK/DEFINE SPACE* reverses the logic to enable transmission of short spaces (i.e. briefly interrupted CW) instead of short pulses. It also reverses the phase of Square pulses, and provides a continuous OFF on CW.

* . Pulses with periods of 5 or 30 secs. cannot be Square.

The BINARY CLOCK controls: *DEFINE MARK/DEFINE SPACE, PULSE REPETITION, PULSE LENGTH* and the LED labelled *MARK*, do not control (or indicate) the *XMITR KEY* state except when the three position switch on the PULSE SEQUENCE PROGRAMMER is set to *BINARY CLOCK*. Consequently these controls can be preset during (say) a MORSE program if desired.

Pulse Sequence Mode

The twelve pulse sequence programs (given below) are selected by the rotary switch labelled *PROGRAM* on the PULSE SEQUENCE PROGRAMMER panel. Six of these programs have a 60 second cycle time and automatically start and reset at U.T. minutes. Four have a 10 second cycle time and two have a 30 second cycle time, but all start and remain synchronised with U.T. (and hence with Dunedin). Changing either this rotary switch or the three position switch at the top automatically resets the phase. Thus switching from programme 5 to programme 6 immediately stops programme 5 but does not start programme 6 (which has a 60 second cycle) until 00 sec. U.T. (minute mark).

NOTE: Programmes 7-12 reset to a mark (or transmitter ON condition).

Program 1

Double pulses of length $1/16$, $1/8$, $1/4$, $1/2$ sec. at 0, 2, 4, 6 sec. U.T. (recycle at 10, 20, ... U.T.) respectively. For each double pulse the mark, space, mark durations are all equal ("square"). The programme is defined in the notation: (0, $1/16$, $1/8$, $3/16$, 2, $2\ 1/8$, $2\ 1/4$, $2\ 3/8$, 4, $4\ 1/4$, $4\ 1/2$, $4\ 3/4$, 6, $6\ 1/2$, 7, $7\ 1/2$, 10 = 0),

where bold type indicates a turn ON or leading edge in seconds U.T. and ordinary type indicates a turn OFF or trailing edge. The last entry (10 = 0) indicates the recycle at 10 sec.

Program 2

A long "pump" pulse (30 sec.) is immediately followed by a series of pulses of increasing length: 1/16, 1/8, 1/4, 1/2, 1, 2, 2, and then by a 20 sec. space to the end of the U.T. minute. Transition times, in the notation above, are:

(0, 30, 30 1/16, 30 1/8, 30 1/4, 30 3/8, 30½, 30 3/4, 31, 31½, 32, 33, 34, 36, 38, 40, 60 = 0).

Program 3

Double pulses each of length ¼ sec. but of increasing separation:

1/4, 1/2, 1 sec. Transition times are:
(0, 1/4, ½, 3/4, 2, 2 1/4, 2 3/4, 3, 5, 5 1/4, 6 1/4, 6½, 10 = 0).

Program 4

Double pulses of form: long pulse, ¼ sec. space, ¼ sec. pulse. For the four double pulses the long pulse has length ½, 1, 2, 5 sec. respectively. (0, ½, 3/4, 1, 5, 6, 6 1/4, 6½, 10, 12, 12 1/4, 12½, 20, 25, 25 1/4, 25½, 30 = 0).

Program 5

Double "square" (equal mark/space/mark) pulses of length 1, 2, 5 sec at 0, 10, 25 sec. U.T. (recycle at 60 sec.) respectively.

It is a continuation of the philosophy of program 1. (0, 1, 2, 3, 10, 12, 14, 16, 25, 30, 35, 40, 60 = 0).

Program 6

Eight single pulses of duration $1/16$, $1/8$, $1/4$, $1/2$, 1, 2, 5, 10 sec. at times (U.T.) 0, 2, 5, 10, 15, 20, 30, 40 sec. respectively. (0, $1/16$, 2, $2\ 1/8$, 5, $5\ 1/4$, 10, $10\ 1/2$, 15, 16, 20, 22, 30, 35, 40, 50, 60 = 0).

NOTE: Programs 7-12 are mark/space inversions of programmes 1-6 respectively. Transition times are the same as given above except that bold figures should be read as turn OFF times and ordinary figures as turn ON times. These "inverted" programmes have interesting properties for investigation of emission triggering and modulation instability.

Program 7 (= 1̄)

Pulses centred in transmission gaps of increasing length: $3/16$, $3/8$, $3/4$, $1\ 1/2$ sec.

Program 8 (= 2̄)

Pulses of increasing length: $1/16$, $1/8$, $1/8$, $1/4$, $1/2$, 1, 2, 20 sec. beginning at 30 sec. U.T., and followed by 30 sec "rest" (space).

Program 9 (= 3̄)

Pulses of length $1/4$, $1\ 1/4$, $1/2$, 2, 1, $3\ 1/2$ sec. respectively (or double $1/4$ sec. gaps of increasing separation).

Program 10 (= 4)

Double pulses of the form: $\frac{1}{4}$ sec. pulse, $\frac{1}{4}$ sec. space, long pulse. For the four double pulses the long pulse has length 4, $3\frac{1}{2}$, $7\frac{1}{2}$, $4\frac{1}{2}$ sec. respectively.

Program 11 (= 5)

Pulses centred in transmission gaps of increasing length: 3, 6, 15 sec.

Program 12 (= 6)

Eight transmission breaks of increasing duration: $\frac{1}{16}$, $\frac{1}{8}$, $\frac{1}{4}$, $\frac{1}{2}$, 1, 2, 5, 10 sec.

Since manual switching produces resetting, make program changes just *before* the U.T. minute to avoid unwanted breaks (e.g. programs 1 and 5 may be used alternately in the sequence 1, 1, 1, 1, 5, 1, 1, 1, ... without breaks by changing during the $2\frac{1}{2}$ "window" $57\frac{1}{2}$ - 60 sec. U.T.).

This pulse sequence program controls the XMTR KEY only when the PULSE/MORSE/BINARY CLOCK switch is set to *PULSE*, so the *PROGRAM* switch can be preset if desired. On switching to *PULSE* (preferably a little before a U.T. minute, since a reset will occur) the LED near the *PROGRAM* switch will light continuously, the LED labelled *MARK* near the top of this panel will light during the ON states (TTL "true") of the XMTR KEY.

slow rate, the first "dot" of H starts 30 seconds after the next 10 sec. pulse after manual switching and the last "dash" (T) is not completed until nearly three minutes after switching.

Sweep Mode

Set the H.P. synthesiser frequency to 200 Hz *above* the desired transmission frequency (f_T) (i.e., set to 21.2 kHz, 19.3 kHz, etc.). Plug H.P. synthesiser into *INPUT* (front panel) and your transmitter input into *OUTPUT*. The *amplitude* of this *OUTPUT* signal will be the same as the *INPUT* to within a few percent (few tenths of dB). The *frequency* of this signal will sweep from $f_T + 46.56$ Hz to $f_T - 46.56$ Hz (e.g. 21.04656 kHz to 20.95344 kHz), in 5 seconds, beginning each sweep at 00, 05, 10, ... seconds U.T.

Turn *PULSE REP.* switch to CW or turn on transmitter ("key down") manually.

NOTE: The instructions called out here are similar to those that would have to be followed by a payload specialist on Spacelab.